Theory and Applications of Mathematics & Computer Science

(ISSN 2067-2764, EISSN 2247-6202)
http://www.uav.ro/applications/se/journal/index.php/tamcs

Theory and Applications of Mathematics & Computer Science 7 (2) (2017) 81 – 123

Proximal Čech Complexes in Approximating Digital Image Object Shapes. Theory and Application

M.Z. Ahmad[a], James Peters[a,b,*]

[a]*Computational Intelligence Laboratory, Department of Electrical & Computer Engineering, University of Manitoba, Winnipeg, MB, R3T 5V6, Canada.*
[b]*Department of Mathematics, Faculty of Arts and Sciences, Adıyaman University, Adıyaman, Turkey.*

Abstract

This article introduces proximal Čech complexes in approximating object shapes in digital images. The theoretical framework is based on Čech complexes and proximity spaces. Several topological structures are defined for the Čech nerve based covers of a finite region of Euclidean plane. We define *k*-petals and *k*-corollas which are the generalizations of spokes and maximal nuclear clusters. We extend the classical notion of a proximity as a binary relation, to arbitrary number of sets. A new shape signature based on the distribution of orders of Čech nerves is defined. A practical application of this framework in approximating object shapes in digital images is given.

Keywords: Čech complex, Digital image, Nerve, Object shape
2010 MSC No: Primary 54E05 (Proximity), Secondary 68U05 (Computational Geometry)

1. Introduction

Understanding of shapes of objects in images is an important aspect of artificial intelligence, with numerous applications. Some of the applications detection of specific patterns in images (Hettiarachchi *et al.*, 2014), quantifying information content of images using Vorono ï tessellations (A-iyeh & Peters, 2016) and detecting outliers from images of different classes (Shamir, 2013). In this paper we aim to understand the shape of the objects in a digital image, by covering it with sets of known geometrical properties. Moreover, we aim at enriching the conventional notion of shape

*Corresponding author: 75A Chancellor's Circle, EITC-E2-390, University of Manitoba, WPG, MB R3T 5V6, Canada; e-mail: james.peters3@ad.umanitoba.ca, research supported by the Natural Sciences & Engineering Research Council of Canada (NSERC) discovery grant 185986 and Instituto Nazionale di Alta Matematica (INdAM) Francesco Severi, Gruppo Nazionale per le Strutture Algebriche, Geometriche e Loro Applicazioni grant 9 920160 000362, n.prot U 2016/000036.

Email addresses: umaiyeh@myumanitoba.ca (M.Z. Ahmad), James.Peters3@umanitoba.ca (James Peters)

as its contour (as used in the prevalent literature) to include the interior as well. For this purpose we will combine the notions of topology and geometry with proximity spaces.

E. Čech introduced Čech complexes during a seminar at Brno(1936-39) (Čech, 1966, §A.5). Recent works define the Čech complexes as collections of intersecting closed geometric balls of a radius of r (Edelsbrunner & Harer, 2010); (Peters, 2017*a*). In this study we focus on approximating shapes of objects in planar digital images. This leads to the restriction of the Čech complexes to a finite bounded region of the Euclidean Plane. In a recent study some open problems regarding planar shapes(shapes of objects in Euclidean plane) have been posed (Peters, 2017*a*) . The viability of Čech complexes as a method to approximate image object shapes has been shown in (Peters, 2017*b*).

A previous study formulates the notion of an object in the digital image as a topological space (Ahmad & Peters, 2017*a*). The notion of a nerve introduced by Alexandroff (Alexandroff, 1965) has been generalized to the notion of spoke complexes. The basic building blocks of the topology are assumed to be curvilinear triangulations. Another study builds on this notion and studies the covering properties of the curvilinear triangulation using the notion of area and geodesic diameter (Ahmad & Peters, 2017*b*). Moreover, a notion of the frequency of nerves of different order as a possible signature of the image objects was also introduced. The notion of proximity was also defined on triangulated spaces (Ahmad & Peters, 2017*a*) and Čech nerves (Peters, 2017*b*).

The subject of the current study is to extend the topological framework for object spaces formulated in (Ahmad & Peters, 2017*a*) to Čech complexes. In addition to this the framework of assessing the covering properties of nerves and object spaces similar to (Ahmad & Peters, 2017*b*) is also developed. A notion of proximity will be introduced on the resulting object spaces. This yields a relator space of objects in the digital images.

2. Basic Definitions

In this section, we will present some basic definitions. Let $X = \mathbb{R}^2$ be the Euclidean plane then $K \in 2^X$ is a finite bounded region in X. The basic building block of Čech complex is the closed geometric ball,$B_r(x)$, with center $x \in X$ and radius $r > 0$ defined as $B_r(x) = \{y \in X : \|x - y\| \leq r\}$.

In this paper, we will study the topology of the objects in a planar digital image. Let us first define **abstract simplicial complex**.

Definition 1. *(Ghrist, 2014, §2.1) Let S be a discrete set. Then the collection of finite subsets of S represented by X is called an abstract simplicial complex, provided for each $\sigma \in X$, all subsets of σ are also in X. This means that X is closed under this restriction.*

Example 1. *Consider a geometric realization of an abstract simplicial complex in form of collections of triangles. Let us first look at the set $X = \{a, b, c\}$, representing the vertices of a triangle as shown in Fig. 1.1. Then the powerset of all the subsets of the set X is,*

$$2^X = \{\{a\}, \{b\}, \{c\}, \{a, b\}, \{a, c\}, \{b, c\}, \{a, b, c\}\}.$$

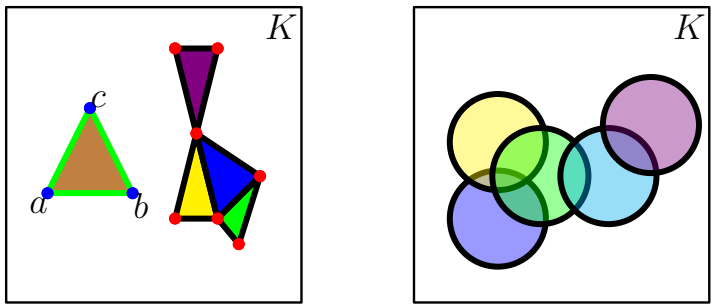

1.1: Collections of triangles 1.2: Collections of Geometric Balls

Figure 1. This figure shows the geometric realizations of abstract simplicial complexes as collections of connected triangles and intersecting closed geometric balls

It can be seen that the set 2^X is closed under restriction as per Def.1. The singleton elements of the set 2^X, i.e. $\{a\}, \{b\}$ and $\{c\}$ represent each of the vertices or the 0-simplices. These are shown in blue on the isolated triangle. The elements $\{a, b\}, \{b, c\}$ and $\{a, c\}$ represent the edges or the 1-simplices. These are shown in green on the isolated triangle. The element $\{a, b, c\}$ represents the filled triangle or the 2-simplex. This is shown with brown color on the isolated triangle. One can easily verify that the connected triangles in Fig. 1.1, also form a simplicial complex. This follows from the fact that each of the triangles in itself is a simplicial complex determined by the power set of the set of its vertices. The whole collection of the triangles is represented by the set Y, which is the union of their respective power sets. Every possible subset of the elements in set Y is contained in itself. Thus set Y is also a simplicial complex as per Def. 1. ■

Keeping in view the previous example it can be seen that the collection of geometric balls($B_r(x)$ for $x \in K$) with a finite number of intersections can be seen as a realization of the abstract simplicial complex. For the purpose of visualization consider the Fig. 1.2 The individual balls are the 0-simplices. The pairs of balls with non-empty intersection are the 1-simplices. The examples are the blue and the violet ball, green and the blue ball etc. If three balls have a common intersection, they lead to a 2-simplex. The yellow, green and blue balls in Fig. 1.2 are an example of a 2-simplex. It can be seen that every pair of balls included in the 2-simplex form a 1-simplex and each constituent ball of this resulting 1-simplex is a 0-simplex. Hence, the collection of closed geometric balls ($B_r(x)$, $x \in K$) is also a geometric realization of an abstract simplicial complex. The 1-simplex which is a line segment in the simplicial complex, is analogous to two Čech balls having common intersection. The 2-simplex is a triangle in the simplicial complex and three Čech balls with a common intersection, in the Čech complex.

Moreover, it can be seen from Fig. 1.2 that one can draw analogs between the simplicial complex (generalization of a triangle to arbitrary dimensions) and the simplices in a Čech complex. It can be seen that each ball in a Čech complex is a 0-simplex and hence similar to the vertex in a simplicial complex. Let us define the notion of a Čech nerve.

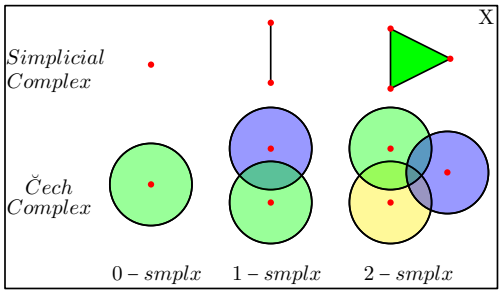

2.1: Comparison of corresponding simplices in a simplicial complex and Čech complex

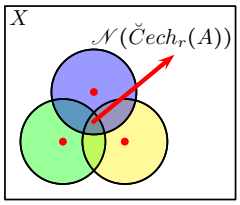

2.2: Nucleus of a Čech nerve

Figure 2. This figure explains the notion of a Čech complex(Def. 3) and compares it with the simplicial complex. Moreover, the notion of the nerve (Def. 11) of a Čech complex is illustrated.

Definition 2. *A **Čech nerve**, is a collection of sets having a non-empty intersection denoted by $(\check{C}ech_r(K))$ i.e.,*

$$\check{C}ech_r(K) = Nrv\{B_r(x) : x \in K\} = \{B_r(x) : \bigcap B_r(x) \neq \varnothing\}.$$

Then, we can define the notion of the **order** of a nerve. It is denoted by $|\check{C}ech_r(K)|$, and is defined as the number of balls in the nerve. We define a set with no non-empty intersections as being a nerve of order 1. Using this notion, we can formulate a definition of the Čech complex in a space X.

Definition 3. *Let X be a finite, bounded planar region $X \in \mathbb{R}^2$ and let $K \in X$ be a nonempty collection of points. A Čech complex is a collection of Čech nerves. The Čech nerves, $\check{C}ech_r(x \in K)$ of order k, form the $k-1$-simplices. The Čech complex is denoted by $cxK = 2^{\check{C}ech_r(K)}, K \in 2^{\mathbb{R}^2}$.*

The basic building block of a Čech complex is a closed geometric ball $B_r(x)$. The view of a digital image as a topological space has been detailed in (Peters, 2014). In current work we extend the conventional notion of a Čech nerve as follows.

Definition 4. *A **strong Čech nerve**, denoted by $\check{C}ech_r^s(K)$, is a collection of sets whose interiors have a non-empty intersection i.e.,*

$$\check{C}ech_r^s(K) = Nrv^s\{B_r(x)"x \in K\} = \{B_r(x) : \bigcap int(B_r(x)) \neq \varnothing\}.$$

In doing so we have also extended the classical notion of a **nerve** to **strong nerve**. A strong nerve is a collection of sets, whose interiors have a non-empty intersection. The notion of **order** remains unchanged. Similar to the notion of the Čech complex, we define the concept of a **strong** Čech complex on a space X.

Definition 5. *Let X be a finite, bounded planar region $X \in \mathbb{R}^2$ and let $K \in X$ be a nonempty collection of points. A strong Čech complex is a collection of strong Čech nerves. The strong Čech nerves, $\check{C}ech_r^s(x \in K)$ of order k form the $k-1$-simplices. The strong Čech complex is denoted by $cx^s K = 2^{\check{C}ech_r^s(K)}, K \in 2^{\mathbb{R}^2}$.*

In this paper we want to approximate the objects in the digital images as topological spaces. This will allow us to talk about shape (Segal & Dydak, 1978) and define invariant signatures for classification (Carlsson *et al.*, 2005); (Chazal *et al.*, 2009). The classical notion of a topology is defined using the notion of open sets.

Definition 6. *(Edelsbrunner & Harer, 2010) Topology is an ordered pair (X, τ), where X is a set and τ is the collection of subsets of X satisfying the following axioms:*
1^o *The empty set, $\varnothing$, and X belong to τ*
2^o *Union of sets in τ is also in τ*
3^o *Intersection of finite number of members of τ is also in τ*

We call this classical notion of topology as **open topology**. Using the De Morgan's laws, we can convert the notion of an open set topology to a closed set topology. Let us define the notion of a complement with respect to a set X. For a set $A \subset X$, the complement of a A denoted by $\overline{A}$ is defined as $\overline{A} = X \backslash A$. The laws state that for two sets A, B:

$$\overline{A \cup B} = \overline{A} \cap \overline{B}$$
$$\overline{A \cap B} = \overline{A} \cup \overline{B}$$

A set A is closed in a topology τ, if its complement $\overline{A}$ is in τ. Using these notions we can extend the definition of a topology with open set as a primitive to using the closed set as the basis. Let us define the notion of topology using closed sets as primitive. To differentiate this we call it a **closed topology**.

Definition 7. *Topology is an ordered pair (X, η), where X is a set and η is the collection of subsets of X satisfying the following axioms:*
1^0 *The empty set, $\varnothing$, and X are closed and belong to η*
2^0 *The intersection of any collection of sets in η is closed*
3^0 *The union of a collection of finite number of sets in η is closed*

Example 2. *Let us examine the equivalence of the two definitions of topology based on open sets(Def. 6) and closed sets(Def. 7). It must be noted that as we have defined the set to be closed under the topology if its complement is in the topology. To establish the equivalence of the notions of open and closed topology we define the collections of subsets η to contain the complement of each subset in the collection τ. This complement is taken with respect to the set X. Let us begin with the first axiom in Def. 6. It states that both the $\varnothing$ and X are in τ. Thus, both are open sets. It can be seen that $\overline{\varnothing} = X \in \tau$ and $\overline{X} = \varnothing \in \tau$. Which means that both $\varnothing, X$ are closed and are in η. Thus, this statement is equivalent to the first axiom stated in Def. 7.*

The second axiom in the Def.6 can be stated as $\{\bigcup_{i\in\mathscr{J}} A_i : A_i \in \tau\} \in \tau$, *where* $\mathscr{J}$ *is an index set which can be infinite and* $A_i \in \tau$. *This means that* $\{\bigcup_{i\in\mathscr{J}} A_i\}$ *is an open set. Which is equivalent to* $\overline{\bigcup_{i\in\mathscr{J}} A_i} \in \eta$ *being a closed set. Using De Morgan's law we can write this as* $\bigcap_{i\in\mathscr{J}} \overline{A_i}$, *where* $\overline{A_i} \in \eta$ *and* $\mathscr{J}$ *is an index set which can be infinite. Since the complement of an open set must be closed,* $\bigcap_{i\in\mathscr{J}} \overline{A_i}$ *must be closed. We have the second axiom of Def. 7. Which states that intersection of any collection of sets in* η *is closed.*

The third axiom in Def. 6 is $\{\bigcap_{i\in\mathscr{J}} A_i : A_i \in \tau\} \in \tau$, *where* $\mathscr{J}$ *is a finite index set. This means that* $\bigcap_{i\in\mathscr{J}} A_i$ *is an open set and its complement is closed. Thus* $\overline{\bigcap_{i\in\mathscr{J}} A_i} = \{\bigcup_{i\in\mathscr{J}} \overline{A_i} : \overline{A_i} \in \eta\}$ *(using De Morgan's law), is a closed set. This statement is equivalent to the third axiom of Def. 7, which states that the union of a collection of finite number of sets in* η *is closed. Hence, the Def. 6 and Def. 7 are equivalent. The former uses the open sets as the primitive and the later uses the notion of a closed set.* ■

Let us define a topology on the Euclidean plane($\mathbb{R}^2$) using the closed geometric balls , $B_r(x)$.

Definition 8. *Let* U *be a closed subset of* $\mathbb{R}^2$ *and* τ_{std} *be a family of closed subsets of* $\mathbb{R}^2$. *Then,* $U \in \tau_{std}$ *if and only if for all* $p \in U$, *there exists a positive real number* r *such that* $B_r(p) \subseteq U$.

Now, let us verify that $(\mathbb{R}^2, \tau_{std})$ is a closed topological space.

Lemma 1. *The pair* $(\mathbb{R}^2, \tau_{std})$ *is a closed toplogical space.*

Proof. Let us verify that the family of subsets τ_{std} satisfies the axioms stated in Def. 7.

1^o : Let us verify that $\varnothing \in \tau_{std}$. From Def. 8, if $\varnothing \in \tau_{std}$, then the following condition must be satisfied.

$$\forall p \in \varnothing \Rightarrow \exists r \in \mathbb{R}^+ \, s.t. \, B_r(p) \subseteq \varnothing$$

It is evident from the definition of implication($\Rightarrow$), that $A \Rightarrow B$ is always true if A is false. Since, $p \in \varnothing$ is always false,thus the statement

$$\exists r \in \mathbb{R}^+ \, s.t. \, B_r(p) \in \varnothing,$$

is true. From this it follows that $\varnothing \in \tau_{std}$. Let us now verify that there exists a positive real number r such that $B_r(x) \subseteq \mathbb{R}^2$, for all $x \in \mathbb{R}^2$. It can be seen from the definition of $B_r(x) = \{y \in \mathbb{R}^2 : \|x - y\| \leq r\}$ that $B_r(x) \subseteq \mathbb{R}^2$ independent of x and r. Thus $\mathbb{R}^2 \in \tau_{std}$.

2^o : Let $\{C_i\}_i$ be a family of sets such that $\forall i, C_i \in \tau_{std}$. Then, if $p \in \bigcap C_i$ then there exists a positive real number r_i for each C_i, such that $B_{r_i}(p) \subseteq C_i$. It can be stated that,

$$B_{r_1}(p) \subseteq C_1 \wedge \cdots \wedge B_{r_i}(p) \subseteq C_i.$$

Let us define $r = \min_i(r_i)$. Then it can be seen that,

$$B_r(p) \subseteq B_{r_1}(p) \subseteq C_1 \wedge \cdots \wedge B_r(p) \subseteq B_{r_i}(p) \subseteq C_i.$$

From this we can conclude that $B_r(p) \in \bigcap C_i$. Therefore, $\bigcap C_i \in \tau_{std}$.

3^o : Let $\{C_i\}_i$ be a finite collection of sets such that $\forall i, C_i \in \tau_{std}$ and $p \in \bigcup C_i$. Then $p \in C_i$, for some i. Since, $C_i \in \tau_{std}$:

$$\exists r \in \mathbb{R}^+ \, s.t. \, B_r p \subseteq U \subseteq \bigcup C_i.$$

From this we can conclude that $\bigcup C_i \in \tau_{std}$.

Thus, it can be concluded that $(\mathbb{R}^2, \tau_{std})$. □

Remark 1. *The notion of a closed standard topology is important as it is the closed set analouge of the standard topology, used for analysis and the conventional signal and image processing.*

Moving on, we define the notion of the closed subset topology.

Definition 9. *Let (X, τ) be a closed topological space, and S be a closed subset of X, i.e. $S \subseteq X$. Let us define $\tau_S = \{S \cap U \, s.t. \, U \in \tau\}$. Then the pair (S, τ_S) is a topological space where τ_S is the subset topology.*

Let us verify that (S, τ_S) is indeed a topological space.

Lemma 2. *Let (X, τ) be a topological space and let S be a closed subset of X. Then the pair (S, τ_S), where $\tau_S = \{S \cap U \, s.t. \, U \in \tau\}$, is a closed topological space.*

Proof. To prove that the pair (S, τ_S) is a closed topological space it must satisfy the axioms detailed in Def. 9.

1^o : It can be verified from the definition of τ_S, that $S \cap (\varnothing \in \tau) = \varnothing$ is in τ_S. Moreover, it can also be verified from definition of τ_S, that $S \cap (X \in \tau) = S$ is also in τ_S. Thus, both $\varnothing$ and S are in τ_S.

2^o : Let $\{C_i\}_i$ be a collection of sets, such that $\forall i, C_i \in \tau_S$. Then from definition of τ_S it can be inferred that, for each $C_i \in \tau_S$ there exists a set D_i in τ, such that for all i, $S \cap D_i = C_i$. Since τ is a closed topology over the set X,then by Def. 9 the set $\bigcap D_i$ is also in τ. This leads to the conclusion that $(\bigcap D_i) \cap S$ is in τ_S by definition. We can see that $(\bigcap D_i) \cap S$ can be written as $\bigcap(D_i \cap S)$. As, we defined in this argument that $D_i \cap S = C_i$ we can conclude that $\bigcap C_i$ is in τ_S.

3^o : Let $\{C_i\}_i$ be a finite collection of sets, such that for all $i C_i \in \tau_S$. Then from the definition of τ_S, we can infer that for each $C_i \in \tau_S$ there exists a set $D_i \in \tau$, such that $D_i \cap S = C_i$. Since, τ is a closed topology then by definition it satisfies the condition that,$\bigcup D_i$ is in τ. From the definition of τ_S we can conclude that $S \cap (\bigcup D_i)$ is in τ_S. From the distributive laws of set algebra we can rewrite this as $\bigcup(D_i \cap S)$ is in τ_S. We know that $D_i \cap S = C_i$, hence $\bigcup C_i$ is in τ_S.

Since the pair (S, τ_S) satisfies all the axioms it is a closed topological space over S, with a subset topology τ_S. □

Now, let us talk about the Čech complex as a closed topological space.

Theorem 1. *Let $(\mathbb{R}^2, \tau)$, be a closed topological space and let cxK be a Čech complex. Then the pair (cxK, τ_{Cech}) is a closed topological subspace, where τ_{Cech} is the subset topology, defined as $\{cxK \cap U \; s.t. \; U \in \tau\}$.*

Proof. Let us first ascertain that *cxK* is a subset of $\mathbb{R}^2$. This follows from definition as *cxK* is the union of Čech nerves($\check{Cech}_r(K)$) as defined in Def. 3. Moreover, the $\check{Cech}_r(K)$ is a union of closed geometric balls as per Def. 2. Next, we can see that the closed geometric balls are in standard closed topology τ_{std} by definition as there exists a positive real number r such that $B_r(p) \subseteq B_r(x)$ for all p in $B_r(x)$. Since, the closed geometric balls are in τ_{std}, thus by the definition of a closed topology, the union of a finite number of closed geometric balls must also be in τ_{std} i.e. closed. Thus, *cxK* is closed and by the definition it is a subset of $\mathbb{R}^2$. From this and Lemma 2, it can be concluded that given a closed topological space $(\mathbb{R}^2, \tau)$, the pair (cxK, τ_{Cech}), where $\tau_{Cech} = \{cxK \cap U \; s.t. \; U \in \tau\}$, is a topological space, where τ_{Cech} is the subset topology. □

Now that we have a notion of Čech nerves as a topological space, we have to draw a correspondence to the objects in digital images. For this purpose, we use specific points from the image called keypoints. There are several algorithms for selecting such points based on their strength in an appropriate feature spaces (Lowe, 1999); (Bronstein & Kokkinos, 2010); (Aubry *et al.*, 2011); (Bruna & Mallat, 2013); (Alahi *et al.*, 2012). We construct Čech nerves with these keypoints as the centers of the geometric closed balls. We assume that the object under consideration, is the most important part of an image in the feature space. Let us now define the topological structures in the strong Čech nerves, that we are going to use as approximations of the objects in an image. We have used the notion of strong Čech nerves because they allow a more rich set of proximity relations, that we will define later on. The same can be done for the Čech nerves.

The first structure that we are going to define is the notion a petal.

Definition 10. *Let $\check{Cech}^s_r(K)$ be a strong Čech nerve,then each closed geometric ball in the nerve $\check{Cech}^S_r(K)$ is called a petal and is denoted by* **ptl**.

Now, we define the notion of a nucleus.

Definition 11. *Let $\check{Cech}^s_r(K)$ be a strong Čech nerve. Then, the nucleus of the nerve is the common intersection of the constituent sets of the nerve. It is defined as $\mathcal{N}(\check{Cech}^s_r A) = \{\bigcap B_r(x) : B_r(x) \in \check{Cech}^s_r A\}$, where $\check{Cech}^s_r A$ is a strong Čech nerve.*

Example 3. *Let us explain the concept of a strong Čech nerve. For this consider Fig. 2.2. K is a set of points in the finite, bounded region of $\mathbb{R}^2$, shown as red points in the figure. The $\check{Cech}^s_r(K)$ in this illustration is the union of the three geometric balls(blue, green and yellow) centered at the points represented as red dots. Each of the individual balls is the petal(***ptl***) of the $\check{Cech}^s_r(K)$. This is represented as* **ptl**$(\check{Cech}^s_r(K))$. *The common intersection of the nerve is called the nucleus. This is represented as $\mathcal{N}(\check{Cech}^s_r(K))$.* ■

We now generalize the concept of a petal to the notion of a k-petal, defined using a recursive definition.

Definition 12. *Let cx^sA be a strong Čech complex on a finite, bounded region of the Euclidean plane $\mathbb{R}^2$,$\check{C}ech^s_rA$ is a strong Čech nerve,and $k > 0$, $k \in \mathbb{Z}$. Then k-petal is defined as the closed geometric ball $B_r(x)$ that has a nonempty intersection with a $(k-1)$-petal. The 0-petal is the nucleus. This can be formally written as:*

$$\mathbf{ptl}_k = \{B_r(x) \in cx^sA \backslash \{\bigcup \mathbf{ptl}_{k-1}\} : B_r(x) \cap \{\bigcup \mathbf{ptl}_{k-1}\} \neq \varnothing, \mathbf{ptl}_0 = \mathscr{N}(\check{C}ech^s_rA)\}.$$

Here, it is important to mention that the nerve of the highest order in the image is very important for object extraction in digital images (Peters & İnan, 2016). Such a nerve is called the **maximal strong Čech nerve** and is denoted as $\mathbf{max}\check{C}ech^s_r(K)$. The nucleus of the maximal strong Čech nerve is called the **maximal nucleus** and is denoted as $\mathbf{max}\mathscr{N}$. It must be noted that there can be multiple maximal strong Čech nerves in a digital image. In this case the the $\mathbf{max}\check{C}ech^s_r(k)$ is a set of each of the maximal strong Čech nerves, and the $\mathbf{max}\mathscr{N}$ is the set of the nuclei associated with the maximal nerves.

Next, we consider the analogue of a corolla, from Botany. A corolla is a cluster of petals of a flower, typically forming a whorl within the sepals and enclosing the reproductive organs. This construct works well in analyzing the interior of Čech complexes that cover an image object shape.

Definition 13. *Let cxA be a strong Čech complex on a finite, bounded region of the Euclidean plane $\mathbb{R}^2$. Then the k-corolla, denoted as $\mathbf{crl}_k$ is defined as: $\mathbf{crl}_k = \bigcup \mathbf{ptl}_k$.*

Another notion that we will define using the notion of a k-petal is the k-petal chain. It is a sequence of petals, one for each value of k. Each petal has a nonempty intersection with adjacent petals in the chain. This notion is formalized as follows.

Definition 14. *Let cx^sA be a strong Čech complex on a finite, bounded region of Euclidean plane $\mathbb{R}^2$. Then the k-petal chain denoted as $\mathbf{ptlchain}_k$ is defined as:*

$$\begin{aligned} \boldsymbol{k>1} : \mathbf{ptlchain}_k &= \{\bigcup_{\mathscr{I}} A_i : A_i \in \mathbf{crl}_i, A_i \cap A_{i-1} \neq \varnothing, \mathscr{I} = 1, \cdots, k\} \\ \boldsymbol{k=0} : \mathbf{ptlchain}_k &= \mathscr{N}(\check{C}ech^s_rA) \end{aligned}$$

Example 4. *Let us explain the topological structures that we have defined above. Let us first explain the notion of a k-petal($\mathbf{ptl}_k$) defined in Def. 12, using Fig. 3.1. The $\mathbf{ptl}_0$(0-petal) has not been explicitly marked on the figure. It is the intersection of the yellow balls and is also the nucleus of the strong Čech nerve, $\mathscr{N}(\check{C}ech^s_r(K))$. Each of the yellow balls is the $\mathbf{ptl}_1$(1-petal). It is evident form the illustration that each of the green balls has a non-empty intersection with the yellow balls ($\mathbf{ptl}_1$) and no intersection with the nucleus($\mathbf{ptl}_0$). Thus each of the green balls is a $\mathbf{ptl}_2$(2-petal) as per Def. 12. Each of the blue balls has a non-empty intersection with the green balls($\mathbf{ptl}_2$), while has no intersection with the yellow balls($\mathbf{ptl}_1$) and as per Def. 12 are the $\mathbf{ptl}_3$.*

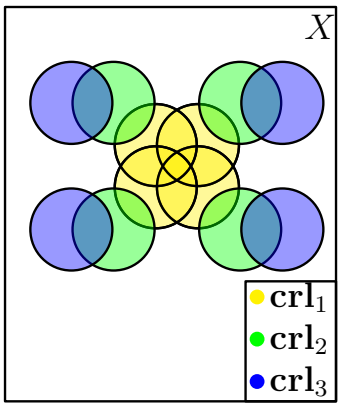

3.1: Collections of triangles

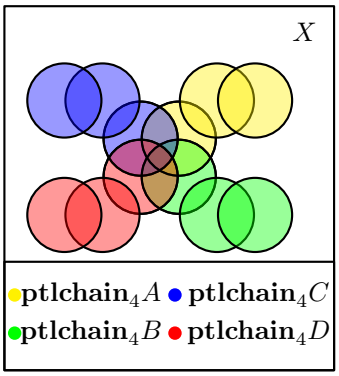

3.2: Collections of Geometric Balls

Figure 3. This figure displays the geometric realizations of the k-corolla, $\mathbf{crl}_k$(Def. 13), and k-petal chain $\mathbf{ptlchain}_k$(Def. 14).

Let us now use the notion of a k-petal to define the notion of a k-corolla($\mathbf{crl}_k$). We are still using the Fig.3.1. The union of all the $\mathbf{ptl}_0$ in the image are the $\mathbf{crl}_0$. Since, there is one nucleus in the image and it has not been marked, hence the $\mathbf{crl}_0$ has not been marked. The union of all the yellow balls ($\mathbf{ptl}_1$) is the $\mathbf{crl}_1$(1-corolla). The union of all the green balls($\mathbf{ptl}_2$) is the $\mathbf{crl}_2$(2-corolla) and the union of all the blue balls($\mathbf{ptl}_3$) is the $\mathbf{crl}_2$(3-corolla) as per Def. 13.

Now using Figs. 3.1 and 3.2 in conjunction, we will explain the idea of a $\mathbf{ptlchain}_k$ (Def. 14). It must be noted that, similar to each of the structures explained in this example, each of the structures has the nucleus of the nerve($\mathcal{N}(\check{C}ech_r^s)$) as its generating point. The $\mathbf{ptlchain}_0$ is the nucleus of the nerve which is the intersection of the yellow balls in Fig. 3.1. It is not labeled in this image. It is important to note here that each of the yellow balls is the $\mathbf{ptlchain}_1$, from Def. 14. This is because it contains the nucleus and the $\mathbf{ptl}_1$(the yellow ball). Thus the $\mathbf{ptlchain}_1$ is the same as the $\mathbf{ptl}_1$. There are four possible $\mathbf{ptl}_1$ and similarly four possible $\mathbf{ptlchain}_1$. Now, by adding to this construction a ball from $\mathbf{crl}_2$, that has a non-empty intersection with the $\mathbf{ptl}_1 \in \mathbf{ptlchain}_1$, we can construct a $\mathbf{ptlchain}_2$ as per Def. 14. In a similar fashion we can construct $\mathbf{ptlchain}_3$ by adding to this construction a ball from $\mathbf{crl}_3$, having non-empty intersection with the $\mathbf{ptl}_2 \in \mathbf{ptlchain}_2$. It can be seen that we can have four possible $\mathbf{ptlchain}_3$ as illustrated in Fig. 3.2. ■

Using the above definitions we will now define the notion of an object space in the strong Čech complex.

Definition 15. *Let cx^sA be a strong Čech complex in a finite, bounded region of an Euclidean plane $\mathbb{R}^2$,and let $\hat{k} \in \mathbb{Z}^+$ such that $\mathbf{crl}_{\hat{k}} = \varnothing$. Then, the object space $\mathcal{O}_p^{\check{C}ech}$, for each $p \in \mathbf{max}\mathcal{N}$ is defined as:*

$$\mathcal{O}_p^{\check{C}ech} = \{\bigcup_k \mathbf{crl}_k : \mathbf{crl}_0 = p,\ k = 0, \cdots, \hat{k} - 1\}$$

We define the notion of a boundary petal **bdypt**.

Definition 16. *Let $\mathcal{O}_p^{\check{C}ech}$ A be an object space over a finite, bounded region of the Euclidean plane, $\mathbb{R}^2$. Then the boundary petal of the object space, **bdpt**$(\mathcal{O}_p^{\check{C}ech})$ is defined as:*

$$\textbf{bdypt}(\mathcal{O}_p^{\check{C}ech}) = \{x : \forall k\, x \in \textbf{crl}_k \text{ and } x \cap \textbf{crl}_{k+1} = \varnothing\}$$

Now, we introduce a bounding corolla in the object space, denoted as **bdycrl**$(\mathcal{O}_p^{\check{C}ech})$.

Definition 17. *Let $\mathcal{O}_p^{\check{C}ech}$ A be an object space over a finite, bounded region of the Euclidean plane, $\mathbb{R}^2$. Then the bounding corolla of the object space, **bdycrl**$(\mathcal{O}_p^{\check{C}ech})$ is defined as:*

$$\textbf{bdycrl}(\mathcal{O}_p^{\check{C}ech}) = \bigcup \textbf{bdypt}(\mathcal{O}_p^{\check{C}ech})$$

Let us define the notion of a maximal petal chains.

Definition 18. *Let cx^sA be a strong Čech complex, and let $\textbf{ptlchain}_kA$ be a petal chain in cxA. Then, $\textbf{ptlchain}_kA$ is called a maximal chain if $\textbf{ptlchain}_kA \cap \textbf{crl}_{k+1} = \varnothing$. The k for which a petal chain becomes maximal is called the **length** of the chain.*

Remark 2. *Each maximal petal chain(**maxptlchain**$_k$ contains a boundary petal(**bdpt**). This follows directly from Def. 16 and Def. 18.*

Using this notion of a **length** of petal chain, we define the regularity of an object space $\mathcal{O}_p^{\check{C}ech}$.

Definition 19. *Let $\mathcal{O}_p^{\check{C}ech}$ be an object space and A be the set of all the maximal petal chains in the object space. $\mathcal{O}_p^{\check{C}ech}$ is called **regular**, provided the length of all the maximal petal chains in A is the same. The object space is called **irregular** otherwise.*

Example 5. *Two types of object spaces are shown in Fig. 4.1 and 4.2. According to Def. 16, in Fig. 4.1 each of the blue balls(in $\textbf{crl}_3$) is the boundary petal as it has a non-empty intersection with the previous corolla(in $\textbf{crl}_2$) but has no intersection with the with next corolla($\textbf{crl}_4$). This is due to the fact that the next corolla, $\textbf{crl}_4$, is $\varnothing$. In Fig. 4.2 each of the blue balls(in $\textbf{crl}_k$) is the boundary petal as it has an intersection with the previous corolla($\textbf{crl}_{k-1}$), but has no intersection with the next corolla($\textbf{crl}_{k+1}$). In contrast to the Fig. 4.1 the Fig. 4.2 has boundary petals in different corolla($\textbf{crl}_k$). As per Def. 17 the collection of all the blue balls is the bounding corolla(**bdycrl**). From Def. 18 we see that both the figures have three maximal petal chains(**maxptlchain**). In Fig. 4.1 all the maximal chains are of equal length 3, thus from Def. 19, the object space in this figure is regular. In Fig. 4.2 the maximal chains(**maxptlchain**) have different length, two chains having lengths of 3 and one chain of length 2. Thus, according to Def. 19 the object space in the figure is an irregular object.* ■

Let us consider the order of a nerve as a signature for the $\mathcal{O}_p^{\check{C}ech}$. Based on this notion we define the Čech spectrum.

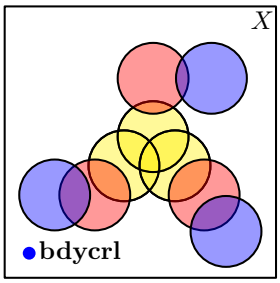

4.1: A regular object space

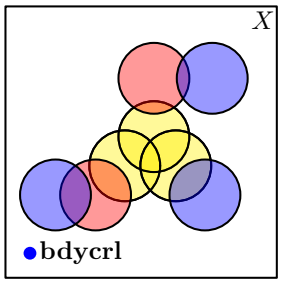

4.2: An irregular object space

Figure 4. This figure illustrates the bounding petal(**bdypt**) defined in Def. 16 and the bounding corolla (**bdycrl**) of an object space defined in Def. 17. Moreover, all the maximal petal chains(**maxptlchain**$_k$) can be identified using the Def. 18 and the accompanying remark. The regularity of an object can be determined using the Def.19

Definition 20. *Let cx^sA be a Čech complex over a finite, bounded region of $\mathbb{R}^2$, Then the Čech spectrum is defined as:*

$$\mathscr{C}(cx^sA) = \{|N^k| : \forall\ k, N^k = \{\check{C}ech_r^s(cx^sA) : |\check{C}ech_r^s(cx^sA)| = k\}\}.$$

It is important to be noted that we count only the unique nerves, i.e. the nerves that are not completely included in a nerve of higher order.

In this paper we study the **proximity** relations defined over the topological structures defined above. **Proximity** is a measure of nearness between non-empty sets, and a non-empty set endowed with a proximity is known as a **proximity space**. The proximity space is represented as a pair (X, δ), where X is a non-empty set and the δ is an arbitrary proximity relation on the set X. In this paper we will use the concept of spatial Lodato proximity(δ), strong proximity($\overset{\wedge\wedge}{\delta}$) and descriptive proximity(δ_Φ). Let us list the axioms of of each of the proximities. We start with the spatial Lodato proximity(δ).

Definition 21. *Let X be a non-empty set and $A, B, C \subset X$ be the subsets of X. Then the spatial Lodato proximity(δ) is a binary relation on the set X, that satisfies the following axioms:*

(P1) $\varnothing \notin A,\ \forall A \subset X.$

(P2) $A\,\delta\,B \Leftrightarrow\ B\,\delta\,A.$

(P3) $A \cap B \neq \varnothing \Rightarrow A\delta B.$

(P4) $A\,\delta\,(B \cup C) \Leftrightarrow A\,\delta\,B\, or\, A\,\delta\,C.$

(P5) $A\delta B\, and\, \forall\ b \in B\,\{b\}\,\delta\,C\ \Rightarrow A\,\delta\,C.$

Now we move on to the definition of strong proximity($\overset{\ggg}{\delta}$).

Definition 22. *Let X be a non-empty set and $A, B, C \subset X$ be the subsets of X. Then the strong proximity($\overset{\ggg}{\delta}$) is a binary relation on the set X, that satisfies the following axioms:*

(snN1) $\varnothing \overset{\ggg}{\not\delta} A,\ \forall A \subset X,$ *and* $X \overset{\ggg}{\delta} A,\ \forall A \subset X.$

(snN2) $A \overset{\ggg}{\delta} B \Leftrightarrow B \overset{\ggg}{\delta} A.$

(snN3) $A \overset{\ggg}{\delta} B \Rightarrow A \cap B \neq \varnothing.$

(snN4) *If $\{B_i\}_{i\in I}$ is an arbitrary family of subsets of X and $A \overset{\ggg}{\delta} B_{i^*}$ for some $i^* \in I$ such that $int(B_{i^*}) \neq \varnothing$, then $A \overset{\ggg}{\delta} (\bigcup_{i\in I} B_i)$.*

(snN5) $intA \bigcap intB \neq \varnothing \Rightarrow A \overset{\ggg}{\delta} B.$

(snN6) $x \in int(B) \Rightarrow x \overset{\ggg}{\delta} A.$

(snN7) $\{x\} \overset{\ggg}{\delta} \{y\} \Leftrightarrow x = y.$

Moving on to the notion of a descriptive proximity(δ_Φ), we first define the notion of a **probe function**. For a set A, the function ϕ maps a feature vector to each of the elements of A. It is defined as $\phi(A) = \{\phi(x) \in \mathbb{R}^n : x \in A\}$. Based on this let us define the concept of a descriptive intersection ($\underset{\Phi}{\bigcap}$). It is defined as $A \underset{\Phi}{\bigcap} B = \{x \in A \bigcup B : \phi(x) \in \phi(A)\ and\ \phi(x) \in \phi(B)\}$. These concepts were introduced and formalized in (Peters, 2007*a*),(Peters, 2007*b*). Let us now formalize the notion of a descriptive proximity(δ_Φ).

Definition 23. *Let X be a non-empty set and $A, B, C \subset X$ be the subsets of the set X. Then the descriptive proximity(δ_Φ) is a binary relation on the set X, that follows the following axioms:*

(dP1) $\varnothing \not\delta_\Phi A,\ \forall A \subset X.$

(dP2) $A \delta_\Phi B \Leftrightarrow B \delta_\Phi A.$

(dP3) $A \underset{\Phi}{\bigcap} B \neq \varnothing \Rightarrow A \delta_\Phi B.$

(dP4) $A\delta_\Phi B\ and\ \{b\}\ \delta_\Phi C,\ \forall b \in B \Rightarrow A \delta_\Phi C.$

Let us build upon the notion a strong proximity($\overset{\ggg}{\delta}$). It is a boolean valued relation i.e. it either tells whether two sets A, B are strongly near($\overset{\ggg}{\delta}$) or strongly far($\overset{\ggg}{\not\delta}$). Next, consider an extension of the Smirnov degree-of-closeness measure (Smirnov, 1952). We define a gradation of the strong proximity to make it a continuous valued function. This then gives a notion of the degree of nearness rather than just an indication of being near or not.

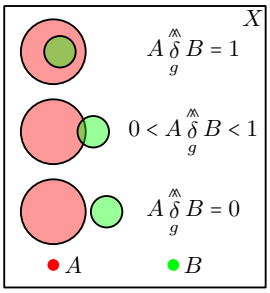

5.1: Gradation of a Strong Proximity

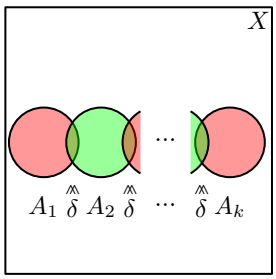

5.2: A sequence in a proximal space

Figure 5. This figure illustrates the gradation of proximity relation. It generalizes the usual binary proximity to a continuous valued relation.Moreover, the concept of a sequence in the procimity space is also illustrated.

Definition 24. *Let X be a non-empty set and $A, B \in X$ be two subsets of X, then we can define a graded strong proximity as a function $\overset{\ggg}{\underset{g}{\delta}} : X \times X \to [0,1]$.*

$$A \overset{\ggg}{\underset{g}{\delta}} B = \frac{|A \cap B|}{min(|A|, |B|)},$$

where $min(a,b)$ returns the smaller of the two numbers.

Remark 3. *It can be seen from the Def. 24, that if $A \overset{\ggg}{\underset{g}{\delta}} B = 0$ then then this means that $A \cap B = \varnothing$, or $A = \varnothing$ or $B = \varnothing$. Any of these conclusions leads to $A \overset{\ggg}{\underset{g}{\not\delta}} B$. Moreover, if $A \overset{\ggg}{\underset{g}{\delta}} B = 1$ then either $A \subseteq B$ or $B \subseteq A$. Thus the graded strong proximity ranges from $\overset{\ggg}{\not\delta}$(for $\overset{\ggg}{\underset{g}{\delta}} = 0$) to $\subseteq$(for $\overset{\ggg}{\underset{g}{\delta}}$=1).*

Let us now talk about a sequence in a proximity space (X, δ).

Example 6. *The notion of proximity as defined in the Def. 22 is a boolean function. This tells us whether two sets are strongly near($\overset{\ggg}{\delta}$) or not($\overset{\ggg}{\not\delta}$). In Def. 24, we define a notion of a continuous valued proximity relation. An illustration of the graded strong proximity is presented in the Fig. 5.1. It can be seen that for the case when $A \cap B = \varnothing$, the strong graded proximity is, $A \overset{\ggg}{\underset{g}{\delta}} B = \frac{0}{min(|A|,|B|)} = 0$. The other extreme of the proximity is when $B \subseteq A$, then $A \overset{\ggg}{\underset{g}{\delta}} B = \frac{|B|}{|B|} = 1$. All the other cases are in between the two extremes, $0 < A \overset{\ggg}{\underset{g}{\delta}} B < 1$, as $0 < |A \cap B| < |B|$. Thus, the graded strong proximity($\overset{\ggg}{\underset{g}{\delta}}$) gives us a more detailed view of the nearness or proximity between two sets.* ■

Definition 25. *Let X be a non-empty set and δ be an arbitrary proximity relation on the set X. Then (X, δ) is a proximity space. Let $A_i \in X$ for $i \in I$, where I is an index set. The a δ-sequence x_n in the proximity space (X, δ) is defined as:*

$$x_n = \{A_i : A_i \delta A_j \; for \, |j - i| \leq 1, \; i, j \in I\}$$

where δ represents the proximity relation.

Let us explain the idea of a sequence in a proximal space.

Example 7. *Let (X, δ) be a proximity space equipped with an arbitrary proximity relation. We define the idea of a sequence which establishes an arrangement of subsets of X. For an illustration of this concept, let us consider Fig. 5.2. It shows a sequence of sets $A_i \subset X$, where $i \in I$, and I is an index set. An important point to note in this definition of a sequence is that a set A_i is proximal only to adjacent sets(A_{i-1}, A_{i+1}) in the sequence and far(not proximal) from all other sets in the sequence. The idea of a δ-sequence can be extended to other proximites such as the $\overset{\curlywedge\curlywedge}{\delta}$ and δ_Φ.* ■

Till now, we have been discussing the notion of proximity as a binary mapping on a set X, of the form $\delta : X \times X \to \{0, 1\}$. Now, let us extend this notion to a mapping of n sets, where n is an arbitrary number. This mapping is termed as a proximity of order n, denoted as δ^n. It is non-continuous surjective map of the form $\delta^n : X^n \to \{0, 1\}$. This generalized notion of a proximity is referred to as **hyper-connectedness**. Let us first define the axioms of a **Lodato hyper-connectedness**. We have used the notation $A\delta B$ to denote that A, B are proximal, and $A \not\delta B$ to denote otherwise. Let us introduce a new notation that will come in handy in the case of hyper-connectedness. If $\delta(A, B, C) = 1$, then A, B are hyper-connected, and if $\delta(A, B, C) = 0$ then the opposite is true.

Definition 26. *Let X be a non-empty set and $\{A_i \subset X : i \in I\}$, where I is an index set, and B, C be the non-empty subsets of X. Let $S(D)$ be the set of n-permutations of the elements of the set D, for $2 \leq n \leq |I|$. Then the spatial Lodato hyper-connectedness(δ^k) is a mapping on k subsets of the set X, that satisfies the following axioms for $k \geq 1$:*

(hP1) $\forall A_k \subset X, \delta^k(A_1, \cdots, A_k) = 0$, *if any* $A_1, \cdots, A_k = \varnothing$.

(hP2) $\delta^k(A_1, \cdots, A_k) = 1 \Leftrightarrow \delta^k(Y) = 1, \; \forall Y \in S(\{A_1, \cdots, A_k\})$.

(hP3) $\bigcap_{i=1}^{k} A_i \neq \varnothing \Rightarrow \delta^k(A_1, \cdots, A_k) = 1$.

(hP4) $\delta^k(A_1, \cdots, A_{k-1}, B \cup C) = 1 \Leftrightarrow \delta^k(A_1, \cdots, A_{k-1}, B) = 1 \, or \, \delta^k(A_1, \cdots, A_{k-1}, C) = 1$.

(hP5) $\delta^k(A_1, \cdots, A_{k-1}, B) = 1 \, and \, \forall b \in B, \, \delta^2(\{b\}, C) = 1 \Rightarrow \delta^k(A_1, \cdots, A_{n-1}, C) = 1$.

(hP6) $\forall A \subset X, \; \delta^1(A) = 1$, *a constant map.*

Now, we use an example to better understand the spatial Lodato hyper-connectedness denoted by δ^k.

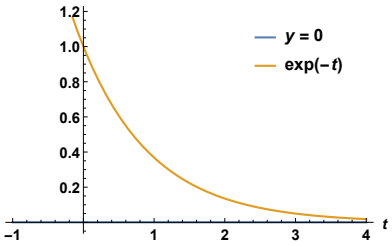

6.1: Lodato Proximity

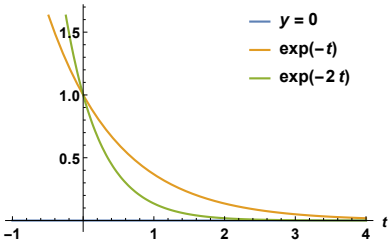

6.2: Lodato hyper-connectedness

Figure 6. This figure illustrates the spatial Lodato proximity in the form of convergence of exponential to the x-axis. It then generalizes this proximity to a hyper proximity, by considering two exponentials converging to x-axis. Further generalization to n such functions follow naturally.

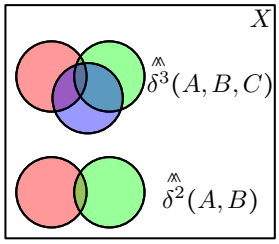

7.1: Strong hyper-connectedness

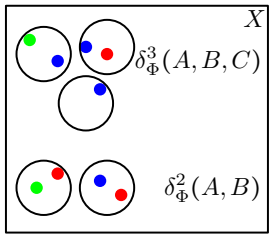

7.2: Descriptive hyper-connectedness

Figure 7. The Fig. 7.1 illustrates the extension of the classical binary relation of spatial Lodato proximity to three sets. Such a relation can be generalized to *n* sets. Fig. 7.2 displays the same for the strong proximity.

Example 8. *Let us consider the idea of a spatial Lodato hyper-connectedness(Def. 26) as illustrated in Fig.6.1. This figure uses two sets* $A = \{y(t) = 0 : \forall t \in \mathbb{R}\}$ *and* $B = \{y(t) = e^{-t} : \forall t \in \mathbb{R}\}$. *It can be observed that these two sets are proximal in the sense that as t approaches* ∞, *the function* e^{-t} *approaches* 0. *Thus* $A \cap B \neq \varnothing$ *in the limit sense. This spatial Lodato hyper-proximity,*δ^2, *for* $k = 2$ *is the classical notion of spatial Lodato proximity defined in Def. 21. Let us extend this idea to arbitrary values of k i.e. to the proximity of k non-empty subsets of a set X. For* $k = 1$, *the notion of a proximity is trivial.* $\delta^1(C) = 1\ \forall C \subset X$ *as every set is proximal to itself. It does not make sense to talk about* $k = 0$ *as there is nothing to quantify the nearness of. Now moving on to* $k = 3$ *as shown in Fig. 6.2. The sets used in this illustration are* $A = \{y(t) = 0 : t \in \mathbb{R}\}$, $B = \{y(t) = e^{-t} : t \in \mathbb{R}\}$ *and* $C = \{y(t) = e^{-2t} : t \in \mathbb{R}\}$. *It is obvious that all the three sets are proximal in the limit sense as the functions* e^{-t} *and* e^{-2t} *approach* 0 *as t approached* ∞. *Thus* $\bigcap(A,B,C) \neq \varnothing$, *which implies that* $\delta^3(A,B,C) = 1$. *Using a similar approach we can generalize this notion for* $k > 3$.

We generalize the notion of strong proximity($\overset{\wedge\wedge}{\delta}$) defined in Def. 21 to the notion of strong hyper-connectedness.

Definition 27. *Let X be a non-empty set and* $A_i, B, C \subset X$ *be subsets of X, where* $i \in I$,*I is an index*

set. Let $S(D)$ be the set of n-permutations of set D, where $2 \leq n \leq |I|$.Then the strong hyper-connectedness($\overset{\wedge\wedge}{\delta^k}$) is a mapping on k subsets of the set X, that satisfies the following axioms for $k \geq 1$:

(snhN1) $\forall A_k \subset X, \overset{\wedge\wedge}{\phi^k}(A_i, \cdots, A_k) = 0$ *if any* $A_1, \cdots, A_k = \varnothing$ *and* $\overset{\wedge\wedge}{\delta^k}(X, A_1, \cdots, A_{k-1}) = 1, \forall A_i \subset X$.

(snhN2) $\overset{\wedge\wedge}{\delta^k}(A_1, \cdots, A_k) = 1 \Leftrightarrow \overset{\wedge\wedge}{\delta^k}(Y) = 1,\ \forall Y \in S(\{A_1, \cdots, A_k\})$.

(snhN3) $\overset{\wedge\wedge}{\delta^k}(A_1, \cdots, A_k) = 1 \Rightarrow \bigcap_{i=1}^{k} A_i \neq \varnothing$.

(snhN4) *If* $\{B_i\}_{i \in I}$ *is an arbitrary family of subsets of X and* $\overset{\wedge\wedge}{\delta^k}(A_1, \cdots, A_{k-1}, B_{i^*}) = 1$ *for some* $i^* \in I$ *such that* $int(B_{i*}) \neq \varnothing$, *then* $\overset{\wedge\wedge}{\delta^n}(A_1, \cdots, A_{k-1}, (\bigcup_{i \in I} B_i)) = 1$.

(snhN5) $\bigcap_{i=1}^{k} intA_i \neq \varnothing \Rightarrow \overset{\wedge\wedge}{\delta^k}(A_1, \cdots, A_k) = 1$.

(snhN6) $x \in \bigcap_{i=1}^{k-1} int(A_i) \Rightarrow \overset{\wedge\wedge}{\delta^k}(x, A_1, \cdots, A_{k-1}) = 1$.

(snhN7) $\overset{\wedge\wedge}{\delta^k}(\{x_1\}, \cdots, \{x_k\}) = 1 \Leftrightarrow x_1 = x_2 = \cdots = x_n$.

(snhN8) $\forall A \in X, \overset{\wedge\wedge}{\delta^1}(A) = 1$ *is a constant map.*

To explain the notion of strong hyper-connectedness we present an example.

Example 9. *Let us consider the illustration of strong hyper-connectedness,$\overset{\wedge\wedge}{\delta^k}$, in the Fig. 7.1. First we consider the case of $k = 2$. The two geometric balls (red and green) have a non-empty intersection and thus $\overset{\wedge\wedge}{\delta^2}(red\ ball, green\ ball) = 1$. Let us now generalize this notion to arbitrary values of k. We consider the case of $k = 1$, which is a trivial case. It can be seen that each ball is strongly near it self. The case of $k = 0$ does not make any sense as the notion of proximity requires a set or an object for definition. Let us now consider the case of $k = 3$. We can see that three geometric balls(red, blue and green) have a non-empty intersection,$\bigcap(red\ ball, green\ ball, blue\ ball) \neq \varnothing$, and thus are strongly proximal. Thus we can write that $\overset{\wedge\wedge}{\delta^3}(red\ ball, green\ ball, blue\ ball)$. Using a similar argument we can extend this notion of strong hyper-connectedness($\overset{\wedge\wedge}{\delta^3}$) to the case of $k > 3$.* ■

Now, we extend the notion of a descriptive proximity to descriptive hyper-connectedness, denoted by δ^k_Φ.

Definition 28. *Let X be a non-empty set and $A_i, B, C \subset X$ be the subsets of the set X, where $i \in I$,I is an index set. Let $S(D)$ be the set of all the n-permutations of set D, where $2 \leq n \leq |I|$. Then the descriptive hyper-connectedness(δ^k_Φ) is a mapping on the set X, that satisfies the following axioms for $k \geq 1$:*

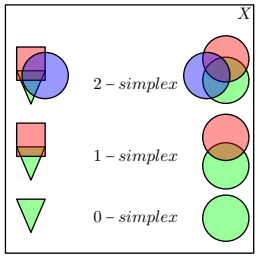

8.1: Hyper-connected complexes

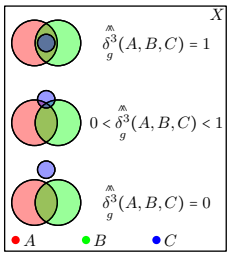

8.2: Graded strong hyper-connectedness

Figure 8. The Fig. 8.1 displays two different hyper-connected complexes defined in a proximity space X. Fig. 8.2 is a graphical visualization of the graded strong proximity for different values in the interval $[0,1]$.

(dhP1) $\forall A_i \subset X,\ \delta^k_\Phi(A_1,\cdots,A_k)=0$ *if any of the* $A_1,\cdots,A_k=\varnothing$.

(dhP2) $\delta^k_\Phi(A_1,\cdots,A_k)=1 \Leftrightarrow \delta^k_\Phi(Y)=1\ \forall Y\in S\left(\{A_1,\cdots,A_k\}\right)$.

(dhP3) $\bigcap\limits_\Phi A_i\neq\varnothing \Rightarrow \delta^k_\Phi(A_1,\cdots,A_k)=1$.

(dhP4) $\delta^k_\Phi(A_1,\cdots,A_{k-1},B)=1$ *and* $\forall b\in B,\ \delta^2_\Phi(\{b\},C)=1 \Rightarrow \delta^k_\Phi(A_1,\cdots,A_{k-1},C)=1$.

(dhP5) $\forall A\subset X, \delta^1_\Phi(A)=1$ *a constant map.*

To help explain the notion of descriptive hyper-connectedness δ^k_Φ.

Example 10. *We use the illustration in Fig. 7.2 to aid in understanding the concept of descriptive hyper proximity(δ^k_Φ). To describe the notion of descriptive proximity we require a probe function $\phi: A\to\mathbb{R}$. In this example we define the probe function such that it returns the hue value(color) of each element of the set. Based on similarity in the hue domain we define the notion of the descriptive proximity(Def. 23). Let us first discuss the case of $k=2$. Consider the two sets at the bottom of the figure. We can see that each has two elements. Now we see that both sets have an element with red color. Thus the sets have a non-empty descriptive intersection i.e. $A\underset{\phi}{\cap}B\neq\varnothing$. This leads to $\delta^2_\Phi(A,B)=1$. Let us now generalize this concept to arbitrary values of k. Now we consider the case of $k=1$. It is obvious that every set is descriptively proximal to itself. Now we can generalize to the case of $k=3$. We can see that the three sets on the top each have an element with blue color. Thus the sets have a non-empty intersection, $\underset{\phi}{\cap}(A,B,C)\neq\varnothing$, which implies that $\delta^3_\Phi(A,B,C)=1$. Using a similar argument we can extend this notion to arbitrary values of k.*

Using the notion of hyper-connectedness, let us define the notion of a hyper-connected complex.

Definition 29. *Let S be a discrete set and X be a collection of non-empty subsets of S. X is a hyper-connected complex,$\delta-cx$, if every collection of non-empty subsets $\{A_1,\cdots,A_n\}\in X$, of cardinality $|n|$, is hyper-connected with respect to a proximity δ i.e. $\delta^n(A_1,\cdots,A_n)=1$. Every subset of size k is the $k-1$ simplex in the resulting hyper-connected complex,$\delta-cx$.*

To clarify the notion of a hyper-connected complex we present the following example.

Example 11. *Let us consider the illustration of a strong hyper-connected complex as depicted in the Fig. 8.1. It can be seen that the bottom row of the figure represents the* 0*-simplex as per Def. 27, we can see that every set is strongly connected to itself. Thus* $\overset{\curlywedge\curlywedge}{\delta}{}^1(A) = 1 \forall A$.

Let us move on to the middle row of the illustration. It can be seen that the two sets are strongly connected thus $\overset{\curlywedge\curlywedge}{\delta}{}^2(A,B) = 1$ *and the remaining constituent sets* $\{A\}$ *and* $\{B\}$ *are also strong hyper-connected(*$\overset{\curlywedge\curlywedge}{\delta}{}^1(A) = \overset{\curlywedge\curlywedge}{\delta}{}^1(B) = 1$*). Thus, the collection* $\{A,B\}$ *is a* 1*-simplex of the strong hyper-connected complex.*

Let us now move to the top row of the illustration. It can be seen that due to the common intersection the $\overset{\curlywedge\curlywedge}{\delta}{}^3(A,B,C) = 1$ *and all of the collections of its subsets are also strongly connected(*$\overset{\curlywedge\curlywedge}{\delta}{}^2(A,B) = \overset{\curlywedge\curlywedge}{\delta}{}^2(A,C) = \overset{\curlywedge\curlywedge}{\delta}{}^2(B,C) = \overset{\curlywedge\curlywedge}{\delta}{}^1(A) = \overset{\curlywedge\curlywedge}{\delta}{}^1(B) = \overset{\curlywedge\curlywedge}{\delta}{}^1(C) = 1$*).Thus the collection of sets* $\{A,B,C\}$ *forms a* 2*-simplex as per Def. 29.*

It must be noted that this concept can be generalized to spatial Lodato hyper-connectedness and descriptive hyper-connectedness.

Let us now define the graded strong hyper-connectedness, denoted by $\overset{\curlywedge\curlywedge}{\underset{g}{\delta}}{}^k$.

Definition 30. *Let* X *be a non-empty set and* $\{A_1, A_2, \cdots, A_n\}$ *be a family of subsets of* X*. Then the graded strong hyper-connectedness is a continuous surjection of the form* $\overset{\curlywedge\curlywedge}{\underset{g}{\delta}}{}: X^n \to [0,1]$ *and is defined as:*

$$\overset{\curlywedge\curlywedge}{\underset{g}{\delta}}{}^k = \frac{|\bigcap(A_1, A_2, \cdots, A_n)|}{min(|A_1|, |A_2|, \cdots, |A_n|}},$$

where $min(a_1, a_2, \cdots, a_n)$ *is the smallest of all the arguments.*

Example 12. *To explain the notion of graded strong hyper-connectedness, denoted as* $\overset{\curlywedge\curlywedge}{\underset{g}{\delta}}{}^k$*, let us consider the Fig. 8.2. Since we are considering three sets we are going to use* $k = 3$ *in the following discussion. First consider the case illustrated towards the bottom of the figure. It illustrates the case when* $\bigcap(A,B,C) \neq \varnothing$ *or any of the* A, B *or* C *is an empty set. In this case the* $\overset{\curlywedge\curlywedge}{\underset{g}{\delta}}{}^3 = 0$ *as per Defn. 30 and the three sets* A, B, C *are not strong hyper-connected,* $\overset{\curlywedge\curlywedge}{\delta}{}^3(A,B,C) = 0$.

Let us move on to the case when there is a partial intersection among the three sets as shown in the illustration in the middle of the figure. We can see that the number of elements in the intersection is smaller than the elements in smallest set i.e. C*. Thus the value of the graded strong hyper-connectedness is between* 0 *and* 1*. The sets* A, B *and* C *are strong hyper-connected(*$\overset{\curlywedge\curlywedge}{\delta}{}^3(A,B,C) = 1$*).*

Let us now consider the third case in which the smallest of the three sets,namely C *is contained in the intersection. This is represented as* $C \subset \bigcap(A,B,C)$*. For this case it can be seen from the*

Def. 30 that $\overset{\curlywedge}{\delta}{}^{3}_{g}(A,B,C) = 1$. *We can extend this framework to higher values of k using a similar argument.* ■

Last, but not the least we present the Borsuk's nerve theorem.

Theorem 2. *(Borsuk, 1948) If U is a collection of subsets in a topological space, the nerve complex is homotopy equivalent to the union of the subsets.*

This theorem will be helpful in the study of Čech object spaces($\mathscr{O}_p^{\check{C}ech}$) undertaken in this paper.

3. Main Results

Lemma 3. *Let* $\mathscr{O}_p^{\check{C}ech}$ *be an object space,* $\boldsymbol{crl}_i \in \mathscr{O}_p^{\check{C}ech}$ *be a corolla,* $\boldsymbol{ptlchain}_k \in \mathscr{O}_p^{\check{C}ech}$ *be a petal chain and* $\hat{k} \in \mathbb{Z}^+$ *such that* $\boldsymbol{crl}_{\hat{k}} = \varnothing$. *Then,* $\bigcup_i \boldsymbol{crl}_i = \bigcup \boldsymbol{maxptlchain}_k$, *where* $i = 0, 1, 2, \cdots, \hat{k} - 1$.

Proof. From Def. 13 it is obvious that $\mathbf{crl}_i = \bigcup \mathbf{ptl}_i$, thus i-corolla is the union of all the i-petals in $\mathscr{O}_p^{\check{C}ech}$. Thus for $i = 0, 1, 2, \cdots, \hat{k}-1$, the $\bigcup_i \mathbf{crl}_i$ is equivalent to $\bigcup_i \bigcup \mathbf{ptl}_i$. Thus, $\bigcup_i \mathbf{crl}_i$, $i = 1, 2, \cdots, \hat{k}-1$, is equal to the union of all the possible $\mathbf{ptl}_i \in \mathscr{O}_p^{\check{C}ech}$($i$-petals in the object space).

Let us now look at Def. 14, from which it can be concluded that each k-petal chain in the object space contains one instance of $\mathbf{ptl}_i \in \mathscr{O}_p^{\check{C}ech}$($i$-petal) for each value $i = 0, 1, \cdots k$. Thus if we consider the $\bigcup \mathbf{ptlchain}_k$, for $k = 0, 1, \cdots, \hat{k} - 1$, we get the union of all the $\mathbf{ptl}_i \in \mathscr{O}_p^{\check{C}ech}$($i$-petal), where $i = 0, 1, \cdots, k$. Which means that union of all $\mathbf{ptlchain}_k \in \mathscr{O}_p^{\check{C}ech}$ consists of all the $\mathbf{ptl}_i \in \mathscr{O}_p^{\check{C}ech}$ for all values of $i = 0, 1, \cdots, k$. Thus, from Def. 13 we get $\bigcup \mathbf{ptlchain}_k = \bigcup_i \mathbf{crl}_i$ for $i = 0, 1, \cdots, k$. From Def. 18 it can be seen that any $\mathbf{ptlchain}_k$ with the largest value of k is called the **maxptlchain**. From Def. 14 it can be seen that every member of the $\mathbf{ptlchain}_k$ has to be a member of the $\mathbf{crl}_i$ in the object space, for all values of $i = 0, 1, \cdots, k$. Thus, the maximum possible value of k for any petal chain can be $\hat{k} - 1$, as $\mathbf{crl}_{\hat{k}} = \varnothing$. It is possible for different maximal petal chains in $\mathscr{O}_p^{\check{C}ech}$ to have different values of k depending on the regularity, as per Def. 19. Keeping this in mind, it is obvious that the $\bigcup$**maxptlchain** equals the union of all the $\mathbf{ptl}_i \in \mathscr{O}_p^{\check{C}ech}$ for $i = 0, 1, \cdots, \hat{k} - 1$.

Thus, we can conclude that both $\bigcup_i \mathbf{crl}_i$ for $i = 0, 1, \cdots, \hat{k} - 1$, and $\bigcup$**maxptlchain** are equal to the union of all the $\mathbf{ptl}_i \in \mathscr{O}_p^{\check{C}ech}$. Hence we can conclude that,$\bigcup_i \mathbf{crl}_i = \bigcup \mathbf{maxptlchain}_k$. □

Using this we can formulate an other definition of the object space($\mathscr{O}_p^{breveCech}$), equivalent to the Def. 15.

Theorem 3. *Let* $cx^s A$ *be a strong Čech complex and an arbitrary positive integer* $\hat{k} \in \mathbb{Z}^+$ *such that* $\boldsymbol{crl}_k \in cx^s A = \varnothing$.*The object space, denoted by* $\mathscr{O}_p^{\check{C}ech}$*(Def. 15), can be defined as:*

$$\begin{aligned}\mathscr{O}_p^{\check{C}ech} &= \{\bigcup_k \boldsymbol{crl}_k : \boldsymbol{crl}_0 = p,\ k = 0, \cdots, \hat{k} - 1\} \\ &= \bigcup \boldsymbol{maxptlchain}.\end{aligned}$$

Proof. From Lemma 3 it can be seen that for $i = 0, 1, \cdots, \hat{k} - 1$, $\bigcup_i \mathbf{crl}_i = \bigcup \mathbf{maxptlchain}_k$. Using this conclusion and Def. 15 it is evident that $\mathscr{O}_p^{\check{C}ech} = \bigcup \mathbf{maxptlchain}$. □

Using this new definition of an object space($\mathscr{O}_p^{\check{C}ech}$), we can comment on the homotopy type of $\mathscr{O}_p^{\check{C}ech}$.

Theorem 4. *The object space $\mathscr{O}_p^{\check{C}ech}$ has the same homotopy type as the union of all the maximal petal chains(**maxptlchain**).*

Proof. From Def. 3 the object space is the union of all the maximal petal chains i.e. $\bigcup$**maxptlchain**. From the Def. 14 we can conclude that every $\mathbf{ptlchain}_k \in \mathscr{O}_p^{\check{C}ech}$ contains the nucleus p which is $\mathscr{N}(\check{C}ech_r^s(A)$. Thus, we can conclude that $\mathscr{O}_p^{\check{C}ech}$ is a nerve as it is union of sets $\bigcup$**maxptlchain**, and the sets have a common intersection $\bigcap$**maxptlchain** $= p$. From Thm. 2, it follows that the homotopy type of the $\mathscr{O}_p^{\check{C}ech}$ is the same as the union of all its **maxptlchain**(maximal petal chains). □

Let us formulate some results for hyper-connectedness relations.

Lemma 4. *Let $C = \{A_1, A_2, \cdots, A_n\}$ be a collection of non-empty subsets of a non-empty set X. If $\delta^n(A_1, A_2, \cdots, A_n) = 1$, then all the possible non-empty sub-collections are also spatial Lodato hyper-connected. This is represented as $\delta^{|T|}(T) = 1$, where T is a sub-collection of the set C.*

Proof. From axiom **(hP2)** of Def. 26, it can be seen that given $\delta^n(A_1, A_2, \cdots, A_n) = 1$(i.e. is Lodato hyper-connected), then all the k-permutations of the elements in the set $\{A_1, A_2, \cdots, A_n\}$ are also Lodato hyper-connected, for $2 \leq k \leq n$. One can see that this axiom is satisfied, provided we introduce an integer $\acute{n} \in \mathbb{Z}^+$, such that $2 \leq k \leq \acute{n} \leq n$. Thus, the axiom is satisfied for all such $\acute{n}$. We have shown that if $\delta^n(A_1, A_2, \cdots, A_n) = 1$, then there exists $\acute{n} \in \mathbb{Z}^+$ *and* $2 \leq \acute{n} \leq n$, such that $\delta^{\acute{n}}(\acute{Y} \in \acute{S}(C)) = 1$. $\acute{S}(C)$ is the set of all the permutations of elements of set C, taken $\acute{n}$ at a time. Now, we need to prove that this equation is also satisfied for subsets of C of size 1. This follows directly from the axiom **(hP6)** of Def. 26, stating that for all $A \in C$, $\delta^1(A) = 1$. Hence, if $\delta^n(A_1, A_2, \cdots, A_n) = 1$, then all non-empty sub-collections($\tilde{C}$) of $C = \{A_1, A_2, \cdots, A_n\}$ also satisfy $\delta^{|\tilde{C}|}(\tilde{C}) = 1$. □

Using the lemma we have just formulated, consider next the following result for spatial Lodato hyper-connected complexes..

Theorem 5. *Let $C = \{A_1, A_2, \cdots, A_n\}$ be a collection of subsets of a non-empty set X, and $\delta^n(C) = 1$. Then C is a spatial Lodato hyper-connected complex($\delta - cx$).*

Proof. From Lemma 4 it follows, that if a collection of sets $C \subseteq X$ satisfyies $\delta^n(C) = 1$, then $\forall T$, $\delta^{|T|}(T) = 1$, where T is a non-empty subcollection of the set C. Thus all possible sub-collections of the set C are also Lodato hyper-connected. From this conclusion and the Def. 29, it directly follows that C is a spatial Lodato hyper-connected complex. Every subset $S \subseteq X$ of size k forms the $k-1$ simplex in the resulting spatial Lodato hyper-connected complex($\delta - cx$). □

Lemma 5. *Let $C = \{A_1, A_2, \cdots, A_n\}$ be a collection of non-empty subsets of a non-empty set X. If $\overset{\curlywedge\curlywedge}{\delta}^n(A_1, A_2, \cdots, A_n) = 1$, then all the possible sub-collections are also strong hyper-connected. This is represented as $\overset{\curlywedge\curlywedge}{\delta}^{|T|}(T) = 1$, where T is a sub-collection of the set C.*

Proof. From axiom **(snhN2)** of Def. 27, it can be seen that given $\overset{\curlywedge\curlywedge}{\delta}^n(A_1, A_2, \cdots, A_n) = 1$(i.e. is strongly hyper-connected), then all the k-permutations of the elements in the set $\{A_1, A_2, \cdots, A_n\}$ are also strongly hyper-connected, for $2 \leq k \leq n$. One can see that this axiom is satisfied, provided we introduce an integer $\acute{n} \in \mathbb{Z}^+$, such that $2 \leq k \leq \acute{n} \leq n$. Thus, the axiom is satisfied for all such $\acute{n}$. We have shown that if $\overset{\curlywedge\curlywedge}{\delta}^n(A_1, A_2, \cdots, A_n) = 1$, then there exists $\acute{n} \in \mathbb{Z}^+$ *and* $2 \leq \acute{n} \leq n$, such that $\overset{\curlywedge\curlywedge}{\delta}^{\acute{n}}(\acute{Y} \in \acute{S}(C)) = 1$. $\acute{S}(C)$ is the set of all the permutations of elements of set C, taken $\acute{n}$ at a time. Now, we need to prove that this equation is also satisfied for subsets of C of size 1. This follows directly from the axiom **(snhN8)** of Def. 22, such that for all $A \in C$, $\overset{\curlywedge\curlywedge}{\delta}^1(A) = 1$. Hence, if $\overset{\curlywedge\curlywedge}{\delta}^n(A_1, A_2, \cdots, A_n) = 1$, then all non-empty sub-collections($\tilde{C}$) of $C = \{A_1, A_2, \cdots, A_n\}$ also satisfy $\overset{\curlywedge\curlywedge}{\delta}^{|\tilde{C}|}(\tilde{C}) = 1$. □

Example 13. *To explain the Lemma 5, let us consider the Fig.7.1. There are two cases of strong hyper-connectedness shown here, namely the $\overset{\curlywedge\curlywedge}{\delta}^2(A, B) = 1$ and $\overset{\curlywedge\curlywedge}{\delta}^3(A, B, C) = 1$.*

*Let us first look at the case of $\overset{\curlywedge\curlywedge}{\delta}^2(A, B) = 1$. Here the set $C = \{A, B\}$ and all the possible sub-collections are $\{A\}$ and $\{B\}$. From axiom **(snhN8)** of Def. 27 it can be seen that $\overset{\curlywedge\curlywedge}{\delta}^1(A) = 1$ and $\overset{\curlywedge\curlywedge}{\delta}^1 B = 1$. Thus, Lemma 5 is satisfied.*

*Now moving on to the case of $\overset{\curlywedge\curlywedge}{\delta}^3(A, B, C) = 1$. Here the set $C = \{A, B, C\}$ and all possible sub-collections can be listed as $\{\{A\}, \{B\}, \{C\}, \{A, B\}, \{B, C\}, \{A, C\}, \{A, B, C\}\}$. We can see that from axiom **(snhN8)** of Def. 27, that $\overset{\curlywedge\curlywedge}{\delta}^1(A) = \overset{\curlywedge\curlywedge}{\delta}^1(B) = \overset{\curlywedge\curlywedge}{\delta}^1(C) = 1$. Moreover, from the figure it can be established that as all the three disks have interior points in common. This leads to the fact that any two of the disks, also have interior points in common. Hence, from axiom **(snhN5)** of Def. 27 $\overset{\curlywedge\curlywedge}{\delta}^2(A, B) = \overset{\curlywedge\curlywedge}{\delta}^2(B, C) = \overset{\curlywedge\curlywedge}{\delta}^2(A, C) = 1$. Hence, Lemma 5 is satisfied.*

The same argument can be extended to higher values of k. ■

From this lemma we obtain the following result.

Theorem 6. *Let $C = \{A_1, A_2, \cdots, A_n\}$ be a collection of subsets of a non-empty set X, and $\overset{\curlywedge\curlywedge}{\delta}^n(C) = 1$, then C is a strong hyper-connected complex($\overset{\curlywedge\curlywedge}{\delta}$ $-cx$).*

Proof. From Lemma 5 it follows, that if the for a collection of sets $C \subseteq X$ satisfying $\overset{\curlywedge\curlywedge}{\delta}^n(C) = 1$, then $\forall T$, $\overset{\curlywedge\curlywedge}{\delta}^{|T|}(T) = 1$, where T is a non-empty subcollection of the set C. Thus all possible sub-collections of the set C are also strong hyper-connected. From this conclusion and the Def. 29, it directly follows that C is a strong hyper-connected complex. Every subset $S \subseteq X$ of size k forms the $k-1$ simplex in the resulting strong hyper-connected complex($\overset{\curlywedge\curlywedge}{\delta}$ $-cx$). □

Lemma 6. *Let $C = \{A_1, A_2, \cdots, A_n\}$ be a collection of non-empty subsets of a non-empty set X. If $\delta^n_\Phi(A_1, A_2, \cdots, A_n) = 1$, then all the possible sub-collections are also descriptivly hyper-connected. This is represented as $\forall\, T$, $\delta^{|T|}_\Phi(T) = 1$, where T is a sub-collection of the set C.*

Proof. From axiom **(dhP2)** of Def. 28, it can be seen that given $\delta^n_\Phi(A_1, A_2, \cdots, A_n) = 1$(i.e. is Lodato hyper-connected), then all the k-permutations of the elements in the set $\{A_1, A_2, \cdots, A_n\}$ are also Lodato hyper-connected, for $2 \leq k \leq n$. One can see that this axiom is satisfied if we introduce an integer $\acute{n} \in \mathbb{Z}^+$, such that $2 \leq k \leq \acute{n} \leq n$. Thus, the axiom is satisfied for all such $\acute{n}$. We have shown that if $\delta^n_\Phi(A_1, A_2, \cdots, A_n) = 1$, then there exists $\acute{n} \in \mathbb{Z}^+$ *and* $2 \leq \acute{n} \leq n$, such that $\delta^{\acute{n}}_\Phi(\acute{Y} \in \acute{S}(C)) = 1$. $\acute{S}(C)$ is the set of all the permutations of elements of set C, taken $\acute{n}$ at a time. Now, we need to prove that this equation is also satisfied for subsets of C of size 1. This follows directly from the axiom **(dhP6)** of Def. 28, that for all $A \in C$, $\delta^1_\Phi(A) = 1$. Hence, if $\delta^n_\Phi(A_1, A_2, \cdots, A_n) = 1$, then all non-empty sub-collections($\tilde{C}$) of $C = \{A_1, A_2, \cdots, A_n\}$ also satisfy $\delta^{|\tilde{C}|}_\Phi(\tilde{C}) = 1$. □

Example 14. *To explain the Lemma 6, let us consider the Fig.7.2. There are two cases of descriptive hyper-connectedness shown here, namely the $\delta^2_\Phi(A, B) = 1$ and $\delta^3_\Phi(A, B, C) = 1$.*

*Let us first look at the case of $\delta^2_\Phi(A, B) = 1$. Here the set $C = \{A, B\}$ and all the possible sub-collections are $\{A\}$ and $\{B\}$. From axiom **(dhP5)** of Def. 28, it can be seen that $\delta^1_\Phi(A) = 1$ and $\delta^1_\Phi B = 1$. Thus, Lemma 5 is satisfied.*

*Now moving on to the case of $\delta^3_\Phi(A, B, C) = 1$. Here the set $C = \{A, B, C\}$ and all possible sub-collections can be listed as $\{\{A\}, \{B\}, \{C\}, \{A, B\}, \{B, C\}, \{A, C\}, \{A, B, C\}\}$. We can see from axiom **(dhP5)** of Def. 28, that $\delta^1_\Phi(A) = \delta^1_\Phi(B) = \delta^1_\Phi(C) = 1$. Moreover, from the figure it can be established that as all the three sets have constituent elements of the same color(blue). This leads to the fact that any two of the sets, will contain constituent elements of same color(blue). Thus, from axiom **(dhP3)** of Def. 28, $\delta^2_\Phi(A, B) = \delta^2_\Phi(B, C) = \delta^2_\Phi(A, C) = 1$. Hence, Lemma 6 is satisfied.*

The same argument can be extended to higher values of k. ■

We now give a result for descriptive hyper-connected complexes..

Theorem 7. *Let $C = \{A_1, A_2, \cdots, A_n\}$ be a collection of subsets of a non-empty set X, and $\delta^n_\Phi(C) = 1$. Then C is a descriptive hyper-connected complex($\delta_\Phi - cx$).*

Proof. From Lemma 6, it follows, that if the for a collection of sets $C \subseteq X$ satisfying $\delta^n_\Phi(C) = 1$, then $\forall T$, $\delta^{|T|}_\Phi(T) = 1$, where T is a non-empty subcollection of the set C. Thus all possible sub-collections of the set C are also descriptivly hyper-connected. From this conclusion and the Def. 29, it directly follows that C is a descriptivly hyper-connected complex. Every subset $S \subseteq X$ of size k forms the $k-1$ simplex in the resulting descriptvly hyper-connected complex($\delta_\Phi - cx$). □

Theorem 8. *Let $A_1, A_2, \cdots, A_n$ be a collection of subsets of a non-empty set X then:*

$1^o: \overset{\curlywedge}{\delta}{}^n(A_1, A_2, \cdots, A_n) \Rightarrow \delta^n(A_1, A_2, \cdots, A_n)$

$2^o: \overset{\curlywedge}{\delta}{}^n(A_1, A_2, \cdots, A_n) \Rightarrow \delta^n_\Phi(A_1, A_2, \cdots, A_n)$

Proof. $1^o:$ It is obvious from axiom **(snhN3)** of Def. 27, that if $\overset{\curlywedge}{\delta}{}^n(A_1, A_2, \cdots, A_n) = 1$, then $\bigcap_{i=1}^{n} A_i \neq \varnothing$. Using this conclusion and axiom **(hP3)** of Def. 26, from $\bigcap_{i=1}^{n} A_i \neq \varnothing$, we can conclude that $\delta^n(A_1, A_2, \cdots, A_n)$.

2^o : From axiom **(snhN3)** of Def. 27, that if $\overset{\curlywedge\curlywedge}{\delta}^n(A_1, A_2, \cdots, A_n) = 1$, then $\bigcap_{i=1}^{n} A_i \neq \varnothing$. Considering $p \in \bigcap_{i=1}^{n} A_i$, we know that $p \in A_i$ for $i = 1, \cdots, n$. If we define a probe function $\phi : X \to \mathbb{R}$, then it is obvious that $\phi(p) \in \phi(A_i)$ for $i = 1, \cdots, n$. Thus $\bigcap_{\Phi} A_i \neq \varnothing$. From axiom **(dhP3)** of Def. 28 it can be concluded that $\delta_{\Phi}^n(A_1, A_2, \cdots, A_n) = 1$.

□

Example 15. *Let us consider the Fig. 7.1, to explain the Thm. 8. It illustrates two cases, namely* $\overset{\curlywedge\curlywedge}{\delta}^2(A, B) = 1$ *and* $\overset{\curlywedge\curlywedge}{\delta}^3(A, B, C) = 1$.

It can be seen that if $\overset{\curlywedge\curlywedge}{\delta}^2(A, B) = 1$, *both the sets* A, B *have interior points in common. Thus, from axiom* ***(hP3)*** *of Def. 26, that* $\delta^2(A, B) = 1$. *The same is true for* $\overset{\curlywedge\curlywedge}{\delta}^3(A, B, C) = 1$. *All the three sets have interior points in common which from axiom* ***(hP3)*** *of Def. 26, leads to* $\delta^3(A, B, C)$.

It can be seen that if $\overset{\curlywedge\curlywedge}{\delta}^2(A, B) = 1$, *both the sets* A, B *have interior points in common. If we consider a probe function* ϕ, *which maps the elements of the sets to a description in* $\mathbb{R}$. *It can be seen that for a point* $p \in A \cap B$, $\phi(p) \in \phi(A) \cap \phi(B)$. *Which means that* $A \bigcap_{\Phi} B \neq \varnothing$.*Thus, from axiom* ***(dhP3)*** *of Def. 28, it can be concluded that* $\delta_{\Phi}^2(A, B) = 1$. *The same is true for* $\overset{\curlywedge\curlywedge}{\delta}^3(A, B, C) = 1$. *All the three sets have interior points in common. Thus for a probe function* ϕ, *if there is a point* $p \in \bigcap(A, B, C)$, *then* $\phi(p) \in \bigcap(A, B, C)$. *Thus* $\bigcap_{\Phi}(A, B, C) \neq \varnothing$. *Thus, from axiom* ***(dhP3)*** *of Def. 28, it can be concluded that* $\delta_{\Phi}^3(A, B, C) = 1$.

This argument can be generalized for higher values of k.

Theorem 9. *Let* $C = \{A_1, A_2, \cdots, A_n\}$ *be a collection of subsets of a non-empty set X, and C is a strong hyper-connected complex i.e.* $\overset{\curlywedge\curlywedge}{\delta}$ *−cx. Then,*

1^o : *C is a* $\overset{\curlywedge\curlywedge}{\delta}$ *−cx* $\Rightarrow$ *C is a* $\delta - cx$

2^o : *C is a* $\overset{\curlywedge\curlywedge}{\delta}$ *−cx* $\Rightarrow$ *C is a* $\delta_{\Phi} - cx$

Proof. 1^o : From Thm. 6 it can be seen that if C is a strong hyper-complex ($sn - cx$), then $\overset{\curlywedge\curlywedge}{\delta}^n(C) = 1$. From Thm. 8 it can be concluded that as $\overset{\curlywedge\curlywedge}{\delta}^n(C) = 1$, then $\delta^n(C) = 1$. From this conclusion and the Thm. 5 it can be concluded that as $\delta^n(C) = 1$, C is a Lodato hyper-complex denoted $\delta - cx$.

2^o : From Thm. 6 it can be seen that if C is a strong hyper-complex ($sn - cx$), then $\overset{\curlywedge\curlywedge}{\delta}^n(C) = 1$. From Thm. 8 it can be concluded that as $\overset{\curlywedge\curlywedge}{\delta}^n(C) = 1$, then $\delta_{\Phi}^n(C) = 1$. From this conclusion and the Thm. 7 it can be concluded that as $\delta_{\Phi}^n(C) = 1$, C is a descriptive hyper-complex denoted $\delta_{\Phi} - cx$.

□

Theorem 10. *A Čech complex is:*

1^o : *spatial Lodato hyper-connected complex,* $\delta - cx$

2^o : *descriptive hyper-connected complex,* $\delta_{\Phi} - cx$

Proof. 1^o : From Def. 3, we come to know that Čech complex is a collection of Čech nerves represented as $\check{C}ech_r(K), K \in \mathbb{R}^2$. Form Def. 2, it can be concluded that $\check{C}ech_r(K)$ is a collection of closed geometric balls,$B_r(x \in K)$, with a non-empty intersection. The $\check{C}ech_rK$ of order k forms the $k-1$ simplex in the Čech complex, as per Def. 3. From the axiom **(dP3)** of Def. 26,it can be concluded that every $k-1$ simplex(or the $\check{C}ech_r(K)$ of order k) is a spatial Lodato hyper-connected collection of sets, i.e. $\delta^{|\check{C}ech_r(K)|}(\check{C}ech_r(K)) = 1$. Using this conclusion and Thm. 5, we can conclude that each $\check{C}ech_r(K)$ is a $\delta - cx$, i.e. a spatial Lodato hyper-connected complex. Similar to the simplicial complex, the union of spatial Lodato hyper-connected complexes is also a spatial Lodato hyper-connected complex.

2^o : From Def. 3, we come to know that Čech complex is a collection of Čech nerves($\check{C}ech_r(K), K \in \mathbb{R}^2$). Form Def. 2, it can be concluded that $\check{C}ech_r(K)$ is a collection of closed geometric balls,$B_r(x \in K)$, with a non-empty intersection. The $\check{C}ech_rK$ of order k forms the $k-1$ simplex in the Čech complex, as per Def. 3. Consider a probe function $\phi : K \to \mathbb{R}$. From the definition of intersection, it can be concluded that a point $p \in \bigcap B_r(x \in K)$ exists in each of the individual $B_r(x \in K)$. Now, when we map each ball to a feature space using the probe function ϕ, it is evident that $\phi(p) \in \bigcap \phi(B_r(x \in K))$. From this it can be concluded that if $\bigcap B_r(x \in K) \neq \varnothing$, then $\bigcap\limits_{\Phi} B_r(x \in K) \neq \varnothing$. Using this result and from the axiom **(dhP3)** of Def. 28, it can be concluded that every $k-1$ simplex(or the $\check{C}ech_r(K)$ of order k) is a descriptively hyper-connected collection of sets, i.e. $\delta_{\Phi}^{|\check{C}ech_r(K)|}(\check{C}ech_r(K)) = 1$. Using this conclusion and Thm. 5, we can conclude that each $\check{C}ech_r(K)$ is a $\delta_{\Phi} - cx$, i.e. a descriptively hyper-connected complex. Similar to the simplicial complex, the union of descriptively hyper-connected complexes is also a descriptively hyper-connected complex.

□

Remark 4. *The Čech complex is not guaranteed to be a strong hyper-connected complex, $\hat{\hat{\delta}} - cx$. This is evident from the definition Def. 3, as it requires the intersection of closed geometric balls,$B_r(x)$, to be non-empty. Since the balls are closed it is possible for the intersection to be points lying on the boundary of the balls. This leads to the spatial Lodato proximity(δ), spatial Lodato hyper-connectedness(δ^n), descriptive proximity(δ_{Φ}) and descriptive hyper-connectedness (δ_{Φ}^n). However, this does not allow the notion of a strong proximity ($\hat{\hat{\delta}}$) and as a consequence the notion of strong hyper-connectedness($\hat{\hat{\delta}}^n$). For these two notions the intersection must comprise of the interior points only.*

Based on the above observation we restrict the notion of a Čech complex to the notion of a strong Čech complex as defined in Def. 5. Now, we present the following results for the strong Čech complex.

Lemma 7. *A strong Čech complex is a strong hyper-connected complex, $\hat{\hat{\delta}} - cx$.*

Proof. It is obvious from Def.5, that a strong Čech complex is a collection of strong Čech nerves, which are represented as $\check{C}ech_r^s(K)$. From the Def.4, it is evident that the strong Čech nerve is a collection of closed geometric balls, $B_r(x \in K)$, such that their interiors have a non-empty intersection. This can be written as $\check{C}ech_r^s(K) = \bigcap \text{int}(B_r(x \in K)) \neq \varnothing$. From the axiom **(snhN5)**,

it can be concluded that, $\overset{\curlywedge}{\delta}^{|\check{C}ech_r^s(K)|}(\check{C}ech_r^s(K)) = 1$. Using this conclusion and from Thm. 6, it can be concluded that $\check{C}ech_r^s(K)$ is a strong hyper-connected complex, $\overset{\curlywedge}{\delta}-cx$. We have proved that, each strong Čech nerve, $\check{C}ech_r^s(K)$ is a $sn-cx$.The union of simplicial complexes is also a simplicial complex. From the Def. 29 that the hyper-connected complex is a case of a simplicial complex (Def. 1), where the simplices are strong hyper-connected collections of sets. Thus, it follows directly that the union of $\overset{\curlywedge}{\delta}-cx$ is also a $\overset{\curlywedge}{\delta}-cx$. Thus, the collections of strong Čech nerves, or a Čech complex, is a strong hyper-connected complex, $\overset{\curlywedge}{\delta}-cx$. □

Using this lemma, let us formulate the following hyper-connectedness relations for the strong Čech complex.

Theorem 11. *A strong Čech complex, cx^sKis:*
1^o : *spatial Lodato hyper-connected complex, $\delta-cx$*
2^o : *descriptive hyper-connected complex, $\delta_\Phi-cx$*

Proof. 1^o : From Lemma 7, it can be seen that a strong Čech complex, cx^sK is a strong hyper-connected complex, $\overset{\curlywedge}{\delta}-cx$. From Thm. 9 it can be concluded that cx^sK is a spatial Lodato hyper-connected complex, $\delta-cx$.

2^o : From Lemma 7, it can be seen that a strong Čech complex, cx^sK is a strong hyper-connected complex, $\overset{\curlywedge}{\delta}-cx$. From Thm. 9 it can be concluded that cx^sK is a descriptive hyper-connected complex, $\delta_\Phi-cx$.

□

Now, we formulate some importatnt results regarding equipping an object space with proximity relations.

Lemma 8. *Let $(\mathcal{O}_p^{\check{C}ech},\{\delta,\overset{\curlywedge}{\delta},\delta_\Phi\})$ be a proximal relator space, and $\mathbf{crl}_k \in \mathcal{O}_p^{\check{C}ech}$, where $k \in \mathbb{Z}^+$. Assuming $\mathbf{crl}_a \overset{\curlywedge}{\delta} \mathbf{crl}_b$, then*
1^o : $\mathbf{crl}_a \overset{\curlywedge}{\delta} \mathbf{crl}_b \Rightarrow \mathbf{crl}_a\,\delta\,\mathbf{crl}_b$
2^o : $\mathbf{crl}_a \overset{\curlywedge}{\delta} \mathbf{crl}_b \Rightarrow \mathbf{crl}_a\,\delta_\Phi\,\mathbf{crl}_b$

Proof. 1^o : From axiom **(snN3)** of Def. 22, it can be concluded that as $\mathbf{crl}_a \overset{\curlywedge}{\delta} \mathbf{crl}_b$, $\mathbf{crl}_a \cap \mathbf{crl}_b \neq \emptyset$. Using the axiom **(P3)** of Def. 21, we can conclude that as $\mathbf{crl}_a \cap \mathbf{crl}_b \neq \emptyset$, then $\mathbf{crl}_a\delta\mathbf{crl}_b$.

2^o : From axiom **(snN3)** of Def. 22, it can be concluded that as $\mathbf{crl}_a \overset{\curlywedge}{\delta} \mathbf{crl}_b$, $\mathbf{crl}_a \cap \mathbf{crl}_b \neq \emptyset$. Let us consider a point $p \in \mathbf{crl}_a \cap \mathbf{crl}_b$ and a probe function $\phi : \mathcal{O}_p^{\check{C}ech} \to \mathbb{R}$. Then it can be seen that $\phi(p) \in \phi(\mathbf{crl}_a) \cap \phi(\mathbf{crl}_b)$, which leads to the fact that $\mathbf{crl}_a \underset{\Phi}{\cap} \mathbf{crl}_b \neq \emptyset$. Using the axiom **(dP3)** of Def. 23, we can conclude that as $\mathbf{crl}_a \underset{\Phi}{\cap} \mathbf{crl}_b \neq \emptyset$, then $\mathbf{crl}_a\delta_\Phi\mathbf{crl}_b$.

□

Theorem 12. *Let $\mathcal{O}_p^{\check{C}ech}$ be an object space and $\mathbf{crl}_k \in \mathcal{O}_p^{\check{C}ech}$, where $k \in \mathbb{Z}^+$. Let $\hat{k}$ be the value of k such that $\mathbf{crl}_{\hat{k}} = \emptyset$. Then, for $0 \leq j < \hat{k}-1$,*
1^o : $\mathbf{crl}_{j+1} \overset{\curlywedge}{\delta} \mathbf{crl}_j$

2^o : $\boldsymbol{crl}_j \overset{\curlywedge}{\delta} \boldsymbol{crl}_{j-1}$

Proof. 1^o : From Def. 13 it can be concluded that $\mathbf{crl}_{j+1} = \bigcup \mathbf{ptl}_{j+1}$ and $\mathbf{crl}_j = \bigcup \mathbf{ptl}_j$. From the Def. 12 it can be seen that a $\mathbf{ptl}_{j+1}$ is a closed geometric ball $B_r(x) \in (cxK \backslash \bigcup \mathbf{ptl}_j)$, such that $B_r(x) \cap \bigcup \mathbf{ptl}_j \neq \varnothing$. Thus each $\mathbf{ptl}_{j+1}$ has a non-empty intersection with $\bigcup \mathbf{ptl}_j = \mathbf{crl}_j$(Def. 13). Since $\mathbf{crl}_{j+1} = \bigcup \mathbf{ptl}_{j+1}$(Def. 13) and each $\mathbf{ptl}_{j+1} \cap \mathbf{crl}_j \neq \varnothing$, we can conclude that $\mathbf{crl}_{j+1} \cap \mathbf{crl}_j \neq \varnothing$. Here, our choice to use the strong Čech complex(cx^s) rather than the Čech complex(cx) as the basis of topological approximation of the underlying space,comes in handy. From Def. 15 it can be seen that we consider the object space($\mathscr{O}_p^{\check{C}ech}$) to be defined over a strong Čech complex(cx^s). Moreover, we can see from the Def. 12 that the petals are the closed geometric balls in the cx^s, and thus the resulting corolla are a collection of these balls. Moreover, each of the intersections in the cx^s(strong Čech complex) is of the form $\bigcap \text{int}(B_r(x))$, as per Def. 5. Based on this we can conclude that all the intersections in the above argument are also on the interiors of the closed geometric balls. Thus, we can conclude that as the object space is formulated on the cx^s(strong Čech complex), $\text{int}(\mathbf{crl}_{j+1}) \cap \text{int}(\mathbf{crl}_j) \neq \varnothing$. Thus from axiom **(snN5)** of Def. 22, we can conclude that $\mathbf{crl}_{j+1} \overset{\curlywedge}{\delta} \mathbf{crl}_j$.

2^o : The argument for the previous case of $\mathbf{crl}_{j+1} \overset{\curlywedge}{\delta} \mathbf{crl}_j$ extends directly to this case of $\mathbf{crl}_j \overset{\curlywedge}{\delta} \mathbf{crl}_{j-1}$, just by considering a dummy variable $\hat{j} = j + 1$. Thus, the case of the $\mathbf{crl}_{j+1} \overset{\curlywedge}{\delta} \mathbf{crl}_j$ for $0 \leq j < \hat{k} - 1$ becomes $\mathbf{crl}_{\hat{j}} \overset{\curlywedge}{\delta} \mathbf{crl}_{\hat{j}-1}$ for $1 \leq \hat{j} < \hat{k}$. This change in the inequality ensures that we only consider the k-corollas for $0 \leq k < \hat{k}$, thus covering a complete range of corollas.

□

Based on this theorem we formulate the follwing important result for the adjacent corollas in an an object space.

Theorem 13. *Let $(\mathscr{O}_p^{\check{C}ech}, \{\delta, \overset{\curlywedge}{\delta}, \delta_\Phi\})$ be a proximal relator space, where $\boldsymbol{crl}_k \in \mathscr{O}_p^{\check{C}ech}$ and $k \in \mathbb{Z}^+$. Let $\hat{k}$ be the value of k such that $\boldsymbol{crl}_{\hat{k}} = \varnothing$. Then, for $0 < j < \hat{k}$,*

1^o : $\boldsymbol{crl}_{j+1} \overset{\curlywedge}{\delta} \boldsymbol{crl}_j \Rightarrow \boldsymbol{crl}_{j+1}\, \delta\, \boldsymbol{crl}_j$

2^o : $\boldsymbol{crl}_j \overset{\curlywedge}{\delta} \boldsymbol{crl}_{j-1} \Rightarrow \boldsymbol{crl}_j\, \delta\, \boldsymbol{crl}_{j-1}$

3^o : $\boldsymbol{crl}_{j+1} \overset{\curlywedge}{\delta} \boldsymbol{crl}_j \Rightarrow \boldsymbol{crl}_{j+1}\, \delta_\Phi\, \boldsymbol{crl}_j$

4^o : $\boldsymbol{crl}_j \overset{\curlywedge}{\delta} \boldsymbol{crl}_{j-1} \Rightarrow \boldsymbol{crl}_j\, \delta_\Phi\, \boldsymbol{crl}_{j-1}$

Proof. 1^o : We can conclude from Thm. 12, that $\mathbf{crl}_{j+1} \overset{\curlywedge}{\delta} \mathbf{crl}_j$, and then from Lemma 8 we can conclude that $\mathbf{crl}_{j+1} \delta \mathbf{crl}_j$.

2^o : We can conclude from Thm. 12, that $\mathbf{crl}_j \overset{\curlywedge}{\delta} \mathbf{crl}_{j-1}$, and then from Lemma 8 we can conclude that $\mathbf{crl}_j \delta \mathbf{crl}_{j-1}$.

3^o : We can conclude from Thm. 12, that $\mathbf{crl}_{j+1} \overset{\curlywedge}{\delta} \mathbf{crl}_j$, and then from Lemma 8 we can conclude that $\mathbf{crl}_{j+1} \delta_\Phi \mathbf{crl}_j$.

4^o : We can conclude from Thm. 12, that $\mathbf{crl}_j \overset{\curlywedge}{\delta} \mathbf{crl}_{j-1}$, and then from Lemma 8 we can conclude that $\mathbf{crl}_j \delta_\Phi \mathbf{crl}_{j-1}$.

□

Let us move on to discuss some important results regarding sequences in a proximity space (X, δ).

Lemma 9. *Let $(X, \{\delta, \overset{\wedge\wedge}{\delta}, \delta_\Phi\})$ be a proximal relator space, and $A_1, A_2, \cdots, A_n$ be subsets of X. Then, if the collection of sets $C = \{A_1, A_2, \cdots, A_n\}$ is $\overset{\wedge\wedge}{\delta}$-sequence:*

1^o : *C is a $\overset{\wedge\wedge}{\delta}$-sequence $\Rightarrow$ C is a δ-sequence*

2^o : *C is a $\overset{\wedge\wedge}{\delta}$-sequence $\Rightarrow$ C is a δ_Φ-sequence*

Proof. 1^o : If C is a $\overset{\wedge\wedge}{\delta}$-sequence, then from Def. 25 it can be concluded that for all $i = 1, \cdots, n$, $A_i \overset{\wedge\wedge}{\delta} A_j$ for $|j - 1| \leq 1$. Using this conclusion and axiom **(snN3)** of Def. 22, we can establish that $A_i \cap A_j \neq \varnothing$ for $|j - 1| \leq 1$. Using axiom **(P3)** of Def. 21, it can be concluded that $A_i \delta A_j$ for $|j - 1| \leq 1$. Thus from Def. 25, we can conclude that C is a δ-sequence.

2^o : If C is a $\overset{\wedge\wedge}{\delta}$-sequence, then from Def. 25 it can be concluded that for all $i = 1, \cdots, n$, $A_i \overset{\wedge\wedge}{\delta} A_j$ for $|j - 1| \leq 1$. Using this conclusion and axiom **(snN3)** of Def. 22, we can establish that $A_i \cap A_j \neq \varnothing$ for $|j - 1| \leq 1$. Now let us consider a point $p \in A_i \cap A_j$ for $|j - i| \leq 1$ and a probe function $\phi : C \to \mathbb{R}$. It can be seen that $\phi(p) \in \phi(A_i) \cap \phi(A_j)$ for $|j - i| \leq 1$, thus $A_i \underset{\Phi}{\cap} A_j \neq \varnothing$. Using axiom **(dP3)** of Def. 23, it can be concluded that $A_i \delta_\Phi A_j$ for $|j - 1| \leq 1$. Thus from Def. 25, we can conclude that C is a δ_Φ-sequence.

□

Let us now consider the petal chain,$\mathbf{ptlchain}_k$, as a sequence in a proximity space.

Theorem 14. *Let $(\mathscr{O}_p^{\check{C}ech}, \overset{\wedge\wedge}{\delta})$ be a proximal object space and $\mathbf{ptlchain}_k \in \mathscr{O}_p^{\check{C}ech}$,for $k \in \mathbb{Z}^+$, be a petal chain contained in it. Then $\mathbf{ptlchain}_k$ is a $\overset{\wedge\wedge}{\delta}$-sequence.*

Proof. From Def. 14 it can be seen that a $\mathbf{ptlchain}_k$ is a collection of subsets A_i of cx^s (a strong Čech complex). These subsets satify the condition that each $A_i \in \mathbf{crl}_i$ and that $A_i \cap A_{i-1} \neq \varnothing$. Since we consider the strong Čech complex(Def. 5), thus all the intersections of the interiors of the subsets of cx^s are non-empty. Thus we can conclude that $\text{int}(A_i) \cap \text{int}(A_{i-1}) \neq \varnothing$. From axiom **(snN5)** of Def. 22, it can be concluded that $A_i \overset{\wedge\wedge}{\delta} A_{i-1}$. Moreover, subsituting $\hat{i} = i - 1$, we get $A_{\hat{i}+1} \overset{\wedge\wedge}{\delta} A_{\hat{i}}$, thus $A_j \overset{\wedge\wedge}{\delta} A_i$ for $|j - i| \leq 1$. Thus, from the Def. 25 it can be seen that as $\mathbf{ptlchain}_k = \{\bigcup_{\mathscr{I}} A_i : A_i \in \mathbf{crl}_i, A_j \overset{\wedge\wedge}{\delta} A_i \ \ for \ |j - i| \leq 1, i, j \in \mathscr{I}\}$. Hence, $\mathbf{ptlchain}_k$ is a $\overset{\wedge\wedge}{\delta}$-sequence with an additional condition that each $A_i \in \mathbf{crl}_i$. □

Using these results we formulate proximity relations for petal chains($\mathbf{ptlchain}_k$) in an object space($\mathscr{O}_p^{\check{C}ech}$).

Theorem 15. *Let $(\mathscr{O}_p^{\check{C}ech}, \{\delta, \overset{\wedge\wedge}{\delta}, \delta_\Phi\})$ be a proximal relator space, $\mathbf{ptlchain}_k \in \mathscr{O}_p^{\check{C}ech}$ be a petal chain, for $k \in \mathbb{Z}^+$. Then.*

1^0 : *$\mathbf{ptlchain}_k$ is a δ-sequence*

2^0 : *$\mathbf{ptlchain}_k$ is a δ_Φ-sequence*

Proof. 1^o : From Thm. 14 we can see that $\mathbf{ptlchain}_k$ is a $\overset{\curlywedge}{\delta}$-sequence and using Lemma 9 we can conclude that $\mathbf{ptlchain}_k$ is a δ-sequence.

2^o : From Thm. 14 we can see that $\mathbf{ptlchain}_k$ is a $\overset{\curlywedge}{\delta}$-sequence and using Lemma 9 we can conclude that $\mathbf{ptlchain}_k$ is a δ_Φ-sequence.

□

Let, us now move on to defining proximity relations on the whole object space, $\mathscr{O}_p^{\check{C}ech}$.

Lemma 10. *Let $(\mathscr{O}_p^{\check{C}ech}, \overset{\curlywedge}{\delta})$ be a proximal object space and $C = \{\boldsymbol{crl}_k : \boldsymbol{crl}_k \in \mathscr{O}_p^{\check{C}ech} \text{ and } k = 0, 1, 2, \cdots, j\}$ is the set of k-corollas of the object space. Suppose $\hat{k} \in \mathbb{Z}^+$ such that $\boldsymbol{crl}_{\hat{k}} = \varnothing$. Then for $0 < j < \hat{k}$, the collection of subsets C is a $\overset{\curlywedge}{\delta}$-sequence.*

Proof. From Thm. 13 it can be seen that $\mathbf{crl}_{j+1} \overset{\curlywedge}{\delta} \mathbf{crl}_j$ and $\mathbf{crl}_j \overset{\curlywedge}{\delta} \mathbf{crl}_{j-1}$ for $0 < j < \hat{k}$. Thus it can be concluded that $\mathbf{crl}_j \overset{\curlywedge}{\delta} \mathbf{crl}_i$ for $|j - i| \leq 1$ where $0 \leq j, i \leq 1$. From Def. 25 it can be concluded that the set $C = \{\mathbf{crl}_k : \mathbf{crl}_k \in \mathscr{O}_p^{\check{C}ech} \text{ and } k = 0, 1, \cdots, \hat{k}\}$ is a $\overset{\curlywedge}{\delta}$-sequence. □

Let us now extend this result to the object space, $\mathscr{O}_p^{\check{C}ech}$.

Theorem 16. *Let $(\mathscr{O}_p^{\check{C}ech}, \overset{\curlywedge}{\delta})$ be a proximal object space, then the object space i.e. $\mathscr{O}_p^{\check{C}ech}$ is a $\overset{\curlywedge}{\delta}$-sequence.*

Proof. From Def. 15 it can be seen that $\mathscr{O}_p^{\check{C}ech} = \{\bigcup_k \mathbf{crl}_k : \mathbf{crl}_0 = p,\ k = 0, 1, \cdots, \hat{k}\}$, which from the definition of union is equivalent to $\{\mathbf{crl}_i : \mathbf{crl}_i \in \mathscr{O}_p^{\check{C}ech},\ k = 0, 1, \cdots, \hat{k}\}$. Thus, from Lemma 10 it is evident that $\mathscr{O}_p^{\check{C}ech}$ is a $\overset{\curlywedge}{\delta}$-sequence. □

Using this theorem, we detail the following proximity relations on the object space, $\mathscr{O}_p^{\check{C}ech}$.

Theorem 17. *Let $(\mathscr{O}_p^{\check{C}ech}, \overset{\curlywedge}{\delta})$ be a proximal object space, and the $\mathscr{O}_p^{\check{C}ech}$ is a $\overset{\curlywedge}{\delta}$-sequence. Then,*

1^o : *$\mathscr{O}_p^{\check{C}ech}$ is a δ-sequence*

2^o : *$\mathscr{O}_p^{\check{C}ech}$ is a δ_Φ-sequence*

Proof. 1^o : From Thm. 16 it can be concluded that $\mathscr{O}_p^{\check{C}ech}$ is a $\overset{\curlywedge}{\delta}$-sequence and from Lemma 9 it is evident that $\mathscr{O}_p^{\check{C}ech}$ is a δ-sequence.

2^o : $\mathscr{O}_p^{\check{C}ech}$ is a $\overset{\curlywedge}{\delta}$-sequence and from Lemma 9 it is evident that $\mathscr{O}_p^{\check{C}ech}$ is a δ_Φ-sequence.

□

4. Computational Experimentation

In this section, we will consider the applications of the topological structures defined in this paper. The aim of this study is to define a topological framework for approximating and extracting the shapes of objects in a digital image. As discussed earlier we require the choice of a selected keypoints from the image. First, we use the scale invariant feature transform(SIFT) based keypoints defined by Lowe (Lowe, 1999).

9.1: Original Image

9.2: Origianl image pre-processed

9.3: SIFT keypoints

9.4: Cech Nerves of different orders

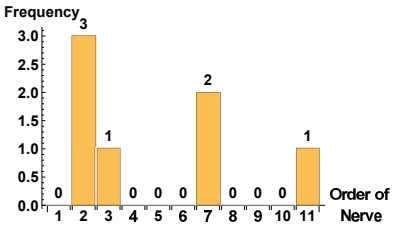

9.5: Cech Spectrum

9.6: 1-Corolla($\mathbf{crl}_1$) of the maximal nerve

Figure 9. This figure displays the image of a boat(Fig. 9.1), and the same image after preprocessing to aid in extracting topological structures(Fig. 9.2). Fig. 9.3 shows the locations of SIFT keypoints. In Fig. 9.4, the Čech nerve are superimposed atop the image. Fig. 9.5 displays the Čech spectrum of the object space, denoted by $\mathscr{C}(\mathscr{O}_p^{\check{C}ech})$. Fig. 9.6 displays the 1-corolla($\mathbf{crl}_1$) of the object space or the maximal Čech nerve.

4.1. SIFT keypoints based Čech complex

Let us first consider the image shown in Fig. 9.1. The main object of focus in this image is a boat. There are many other objects e.g. mountain, beach, sea and people in the image, that can be considered as noise for current application. To aid in approximating the shape of the main object i.e. the boat, we pre-process the image to remove all other objects. The output of this pre-processing is displayed in Fig. 9.2. It can be observed that almost everything apart from the distinctive features of the boat have been removed. Some of the parts of the boat have also been removed because of the similarity with the objects that were considered to be noise.

After the pre-processing stage we extract the SIFT keypoints from the image, represented as a set S. Based on these points we can now construct a Čech complex(Def. 3) by considering a collection of balls of radius r, $\{B_r(s) : s \in S\}$ super-imposed on to the image. Every set of k balls with a non-empty intersection is the $k-1$ simplex in the resulting abstract simplicial complex.

Algorithm 1: Čech Complex represenatation of Image Objects

Input : digital image *img*, Keypoints S, Čech radius r
Output: Čech complex on the image $\check{C}ech_r(S)$,Čech nerve of maximal order **max**$\check{C}ech_r(S)$, Čech spectrum $\mathscr{C}$

foreach $s \in S$ **do**
  $\check{C}ech_r(S) := \check{C}ech_r S \cup B_r(s)$;
/*Calculating the Čech spectrum*/;
$\mathscr{S} := S$;
$Nrv(0) := S$;
Continue ← *True; k* ← *1*;
while *Continue* = *True* **do**
  $\mathscr{S} :=$ *(k + 1)-Combination of S*;
  foreach *comb* $\in \mathscr{S}$ **do**
    bnddsk ← *minimal bounding disk of the (k + 1) points in comb*;
    rad ← *radius of bnddsk*;
    if *rad* $\leq r$ **then**
      nerve ← *comb*;
    else
      */*Continue*/*;
  if *nerve* $\neq \varnothing$ **then**
    $\hat{S}$ ← *all the unique points* $s \in S$ *present in nerve*;
    $Nrv(k-1) := Nrv(k-1) \setminus \{(k) - Combination\ of\ \hat{S}\}$;
    $\acute{S} := S \setminus \hat{S}$;
    $k \leftarrow k + 1$;
  else
    Continue ← *False*;
    maximalorder ← *k*;
$j \leftarrow 1$;
while $j \leq$ *maximalorder* **do**
  $Nrv(j) \longmapsto$ *number of elements*;
  $(j) \leftarrow$ *number of elements*
max$\check{C}ech_r(S) := Nrv(maximalorder)$;
$\check{C}ech_r(S) \longmapsto img$;

Moreover, it can be seen that every set of k geometric balls with a non-empty intersection is called a Čech nerve, denoted by $\check{C}ech_r(S)$. The common intersection is termed as the nucleus and the number of balls k in the nerve is termed its order. An overview of the algorithm to generate the Čech complex is presented in Alg. 1. In Fig. 9.4 all the $\{\check{C}ech_r s : s \in S\}$ in the Čech complex are illustrated on the image. The nerves have been color coded with respect to their order.

Here we can see that for the current choice of radius r, the collection of balls form two complexes as there is no intersection in between them. One of the complexes is on the front side of the boat while the other complex is on the mast and the rear end of the boat. If we increase the radius both these complexes will merge in to one complex. This is an important point to note and is common to this and other frameworks which aim to model the data using topological constructs (Ghrist, 2008). The topological features of the approximation built using Čech and related complexes is dependent on the radius. The appropriate choice of radius will be discussed in a future work.

Here we present a possible topological signature of the shape. It is termed as the Čech spectrum and is defined in Def. 20. It is defined as a sequence of numbers which represents the number of nerves of a particular order in an image. A similar shape signature was considered for the approximation of object space via curved and rectilinear triangulations (Ahmad & Peters, 2017*b*). It can be seen that this is related to the spatial distribution of the keypoint locations and the radius of the geometric balls. Nerves of higher order are a result of a large number of keypoints proximal to each other. Thus, based on how the keypoints are selected the nerves of different order represent different concentrations(or clusters) of specific features in an image. Based on this we can assume that the region in the image, where the highest number of keypoints are mutually proximal is the most important region.

This brings us to the concept of a maximal Čech nerve. For the image under consideration we can see from the Čech spectrum that the order of the maximal nerve is 11 and there is only one of them in the image. Let us look at the location of this nerve on the image. It is shown in Fig. 9.6. We can see that this nerve lies on the saftey tube hanging on the mast towards the rear end of the boat. The reason for this is the the tube is a compact structure that is highly differentiated from its background. Thus there is a high distribution of SIFT keypoints. Moreover, there are keypoints corresponding to the rear hull of the boat. The combination of these points results in the existence of the maximal nerve in this region of the image.

Each of the balls in this image is the maximal nerve is the 1-petal, denoted as $\mathbf{ptl}_1$. The union of all the $\mathbf{ptl}_1$ in the maximal nerve is called the $\mathbf{crl}_1$. Thus the maximal Čech nerve is equivalent to the $\mathbf{crl}_1$. All the geometric balls in the image that has a non-empty intersection with the 1-corolla($\mathbf{crl}_1$) is called the 2-petal, denoted as $\mathbf{ptl}_2$. The union of all the $\mathbf{ptl}_2$ in the image is called the 2-corolla($\mathbf{crl}_2$). The concept can be generalized to higher values of k in a similar fashion. Thus, the image shown in Fig. 9.6 also represents the 1-corolla or the $\mathbf{crl}_1$.

Let us consider the image of a car as shown in the Fig. 10.1. This image contains a black car, with many other objects such as a human, building, partial parts of a car and bus. Thus, the image contains the focal object and a lot of other objects which for the purpose of this study we consider to be noise. After the pre-processing to remove all other objects apart from the focal object we obtain the image shown in Fig. 10.2. We use this image to select keypoints(set S) which will then be used to construct a Čech complex and superimpose it on the image. The nerves in the Čech complex($\{\check{C}ech_r(s) : s \in S\}$) are color coded with respect to number of sets in them(order). This result is shown in Fig. 10.4. In contrast to the result for the image of the boat as shown in Fig. 9.4, we can notice that the collection of all the geometric balls of radius r form a single Čech complex.

Let us now move on to the newly proposed shape signature, namely the Čech spectrum. For the approximation of the shape of the car with Čech complex, the Čech spectrum is displayed in

10.1: Original Image

10.2: Origianl image pre-processed

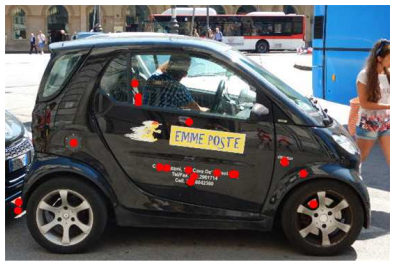

10.3: SIFT keypoints

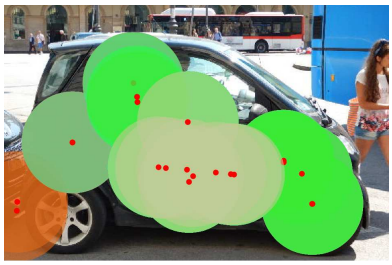

10.4: Cech Nerves of different orders

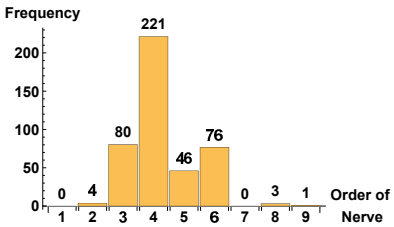

10.5: Cech Spectrum

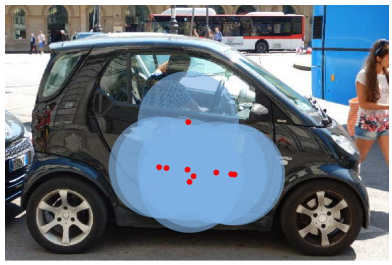

10.6: 1-Corolla($\mathbf{crl}_1$) of the maximal nerve

Figure 10. This figure displays the image of a car (Fig. 10.1), and the same image after preprocessing to aid in extracting topological structures(Fig. 10.2). The keypoints extracted by the SIFT algorithm are shown in Fig. 10.3.In Fig. 10.4, the Čech nerve are superimposed atop the image. Fig. 10.5 displays the Čech spectrum of the object space, denoted by $\mathscr{C}(\mathscr{O}_p^{\check{C}ech})$. Fig. 10.6 displays the 1-corolla($\mathbf{crl}_1$) of the object space or the maximal Čech nerve.

Fig. 10.5. It can also be observed that the Čech spectrum for the car is different from that of the image of the boat(Fig. 9.5). The order of the maximal Čech nerve was 11 for the boat and is 9 for the car. The number of nerves of maximal order is again one. There can be multiple maximal Čech nerves in an image. In that case we can either consider them to be multiple objects or the different(in terms of features) regions in the same image. This choice is dependent on whether we consider our image to contain a single focal object or multiple ones.

We plot the maximal Čech nerve on the image and display it in Fig. 10.6. It can be seen that the maximal nerve lies on the interior of the car on its front door. Moreover, as discussed earlier it the maximal Čech nerve is the same as the 1-corolla($\mathbf{crl}_1$) and each of the balls in it is the 1-petal($\mathbf{ptl}_1$). All the geometric balls that share a non-empty intersection with the $\mathbf{crl}_1$ are called the 2-petals($\mathbf{ptl}_2$). The union of all the 2-petals($\mathbf{ptl}_2$) is called the 2-corolla($\mathbf{crl}_2$). We can extend the concept of *k*-petals and *k*-corolla to this image as we did to the image of the boat.

4.2. Čech complex using hole based keypoints

After discussing the results of approximating the objects in an image using Čech complexes based on SIFT based keypoints, we develop a new type of key points. These types of keypoints are based on the notion of a hole. The notion of a hole is a vital one in topology (Alexandroff, 1965).

Let us consider an extension of this concept to a digital image. We use the notion of a **descriptive hole**, defined as below.

Definition 31. *A descriptive hole is a finite bounded sub-region of a plane with a matching description. The description is obtained by the probe function,* $\phi : 2^X \to \mathbb{R}$.

Algorithm 2: Hole based Keypoints

Input : digital image *img*, Horizontal filter radius r_x, Vertical filter radius r_y, Hole threshold t, Number of holes n_{hole}
Output: Hole locations $\mathscr{K}_{holes}$

$f_G(x,y) := \frac{1}{2\pi r_x r_y} exp(-(\frac{x^2}{2r_x^2} + \frac{y^2}{2r_y^2}))$;
$img_{filt} \leftarrow f_G(x,y) * img$;
$g :=$ *empty matrix*;
foreach *pixel* $\in$ *img* **do**
    $J :=$ *empty matrix*;
    foreach *channel* $\in$ *pixel* **do**
        $J(channel,:) := Grad(pixel)$;
    $(i,j) \leftarrow$ *location of pixel*;
    $g(i,j) \leftarrow \sqrt{\lambda_{max}(J^T J)}$;
$g :=$ *set all values of* $g < t$ *to* 1 *and rest to* 0;
$g \longmapsto$ *connected components*;
connected components $\longmapsto$ *size in terms of pixels*;
/* arrange in descending order w.r.t. size in terms of pixels */;
connected components $\longmapsto$ *arranged connected components*;
hole $\leftarrow$*first* n_{hole} *arranged connected components*;
hole $\longmapsto$ *centroids*;
$\mathscr{K}_{holes} \leftarrow$ *centroids*;

In this paper we consider the description to be the pixel intensity, which for coloured images is a vector of values in domain $\mathbb{R}^n$. Where n is the number of channels in the image. For a classical coloured image, the RGB color image, this is 3. A digital image is represented as a matrix (size $m \times n$) for computation, and for the RGB image this becomes a collection of three matrices or a multi-way array of size $m \times n \times 3$. For the purpose of detecting holes, we first convolve the image with a normalized Gaussian kernel to remove noise. The 2D normalized Gaussian is defined as:

$$f_G(x,y) = \frac{1}{2\pi r_x r_y} e^{-(\frac{x^2}{2r_x^2} + \frac{y^2}{2r_y^2})},$$

where r_x and r_y define the standard deviation of the Gaussian in the x and y direction respectively. The standard deviation dictates the radius of the smoothing filter. This smoothed image

is then used to calculate the derivative for each pixel. The derivative is calculated using the a traditional derivative filter such as the sobel operator. In an image, for each pixel there are two derivative, one in the x and one in the y direction. We combine the derivatives in a Jacobian matrix(J).

To illustrate this concept, let us consider the RGB image to be a map(img) that assigns an intensity($\mathbb{R}^3$) to each pixel location($\mathbb{R}^2$). This is represented as $img : \mathbb{R}^2 \to \mathbb{R}^3$. The Jacobian matrix($J$) for each pixel would thus be a matrix of size 2×3, defined as:

$$J(img(x,y)) = \begin{bmatrix} \frac{\partial img(1)}{\partial x} & \frac{\partial img(1)}{\partial y} \\ \frac{\partial img(2)}{\partial x} & \frac{\partial img(2)}{\partial y} \\ \frac{\partial img(3)}{\partial x} & \frac{\partial img(3)}{\partial y} \end{bmatrix},$$

where $img(i)$ represents the ith channel of the image. The gradient magnitude for each pixel $g(x,y)$ is calculated as:

$$g(x,y) = \sqrt{\lambda_{max}(J(img(x,y))^T J(img(x,y)))},$$

where $\lambda_{max}(A)$ is the larget eigen value of matrix A.

Once, we have the gradient magnitude for each pixel in the image we can then threshold to yield the location of regions with relatively constant pixel intensities. The value of the threshold decides the ammount of variation that we are willing to allow in the description of a hole. Since, we are interested in the areas with a gradient close to 0, we set all the pixels with gradient values less than the threshold to be 1 and the rest to be 0. In this fashion we mark all the regions of interest(or holes as we refer to them) as 1. We can extract these regions using connected component analysis, and then calculate the size of the region in terms of the number of pixels and its centroid. The holes are arranged in the descending order with respect to their size and the hole based keypoints($\mathscr{K}_{hole}$) are the centroids of these holes. The size of the hole is a determinet of its importance in the image. This method is summarized in Alg. 2.

Once, we have the hole-based keypoints, $\mathscr{K}_{hole}$, they are input to the Alg. 1 to build the Čech complex so that features of the objects in the image can be extracted. This process is similar to the one performed for the SIFT keypoints in § 4.1. Let us discuss the application of this new class of keypoints to the images used in § 4.1. Let us first illustrate the location of the new form of keypoints on the image of the boat, as shown in Fig. 11.1. The difference between the objects extracted from the digital images using the two differnet types of keypoints lies in the location of the keypoints. Let us compare the location of the SIFT and hole-based keypoints($\mathscr{K}_{hole}$), shown in Fig. 9.3 and Fig. 11.1 respectivly. We can see that due to the specific construction of $\mathscr{K}_{hole}$, these exist on a region with a constant intensity. It can be seen that in the SIFT based keypoints are located along edges of the main body of the boat, while one of the $\mathscr{K}_{hole}$ lies near the center of the body of the boat. The rest of the keypoints are mostly concentrated near the bottom edge of the boat on the shadow, and the life tube. These objects are very narrow, so the SIFT and the $\mathscr{K}_{hole}$ are at almost similar locations. It is easy to see that for a narrow objects the centeroids are close to the

11.1: Hole-based keypoints

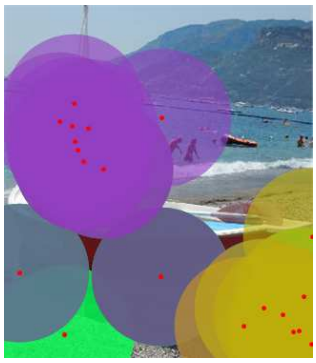

11.2: Čech nerve of different order

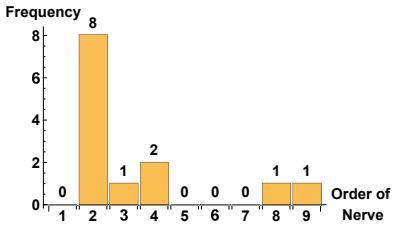

11.3: Čech Spectrum

11.4: Maximal Čech nerve

Figure 11. Fig. 11.1 displays the hole-based keypoints on the original image of the boat. Čech nerves of different order are shown in Fig. 11.2. Fig.11.3 displays the Čech spectrum for the hole-based keypoints. The maximal Čech nerve or the 1-corolla($\mathbf{crl}_1$) is displayed in Fig. 11.4.

edges.

Let us now look at the Čech nerves of differnet order imposed on the image. It is shown in Fig. 11.2 and the nerves are color coded with respect order(the number of geometric balls in the nerve). The radius used to generate this result is the same as that for the SIFT based keypoints shown in Fig. 9.4. It can be seen that Čech nerve generated using $\mathscr{K}_{holes}$ covers more area of the boat, that the Čech nerve generated using the SIFT keypoints.

The Čech spectrum or the number of unique Čech nerves of a specific order in the Čech complex($\check{C}ech_r(K)$) is defined as Def. 20. For the Čech complex generated using the hole-based keypoints, denoted as $\check{C}ech_r(\mathscr{K}_{holes})$, the Čech spectrum($\mathscr{C}$) is displayed in Fig. 11.3. Comparing this with the result for the SIFT keypoints(Fig. 9.5), it can be seen that the Čech spectrum is quite different. It can be seen that the order of the maximal Čech nerve for $\mathscr{K}_{hole}$ is 9, while for the SIFT based case is 11.

One commonality between the Čech complexes for both the SIFT and $\mathscr{K}_{holes}$ is the location of the maximal Čech nerve or the 1-corolla($\mathbf{crl}_1$). Other topological structures can be extracted for the $\mathscr{K}_{holes}$ based $\check{C}ech_r(\mathscr{K}_{holes})$ in the same fashion as for the SIFT based case explained with

12.1: Hole-based keypoints

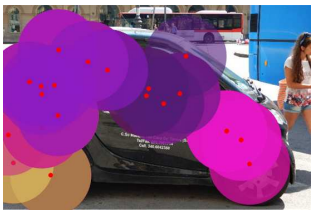

12.2: Čech nerve of different order

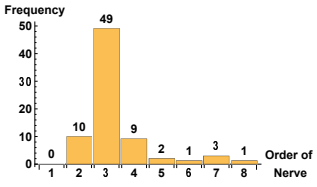

12.3: Čech Spectrum

12.4: Maximal Čech nerve

Figure 12. Fig. 12.1 displays the hole-based keypoints on the original image of the car. Čech nerves of different order are shown in Fig. 12.2. Fig.12.3 displays the Čech spectrum for the hole-based keypoints. The maximal Čech nerve or the 1-corolla($\mathbf{crl}_1$) is displayed in Fig. 12.4.

detail in § 4.1.

Let us move on to the case of extracting the shape of the car using $\mathscr{K}_{holes}$. We consider the location of the SIFT keypoints(Fig.10.3) and compare them with the location of the $\mathscr{K}_{holes}$(Fig. 12.1). For this image it can be seen that the SIFT based keypoints for the image of the car are located in the center of the object on the front door. While, the $\mathscr{K}_{holes}$ for this image are located towards the upper contour of the car. The SIFT points are located on the front door due to the text. There are lot of edges on the front door thus the SIFT based keypoints lie on these edges. Moreover, the location of $\mathscr{K}_{holes}$ are on the rims, the mirros and the bumper of the car on the back. The locations of the keypoints for the SIFT are on the on the text, bottom fender of the car on the back and on the arm of the man in the car. Due to the centrality of the text on the car the SIFT keypoints for this image are concentrated on the center of the car.

This is the main reason for the $\check{C}ech_r(K)$ generated using the SIFT keypoints(Fig. 10.4) cover the car better than the $\mathscr{K}_{holes}$(Fig. 12.2). The nerves of different order are color coded for the Čech complex generated using $\mathscr{K}_{holes}$ are displayed in Fig. 12.2. The Čech complex for the $\mathscr{K}_{holes}$ conforms very well to the top contour of the car and the tires, but the bottom part of the front door remains uncovered. The Čech spectrum of the $\check{C}ech_r(K)$ usig the $\mathscr{K}_{holes}$ is shown in Fig. 12.3. It can be seen that this Čech spectrum is different from the case of the SIFT keypoints shown in Fig. 10.5. The maximal Čech nerve for the $\mathscr{K}_{holes}$ is 8 while for the SIFT keypoints is 9. Moreover the case of the car, the location of the maximal nerver or the 1-corolla($\mathbf{crl}_1$) is also different for the SIFT keypoints and the $\mathscr{K}_{holes}$. For the SIFT the maximal nerve is on the front door while for the $\mathscr{K}_{holes}$ it is on the top of the rear end of the car. This difference is fundamentaly due to the difference in the spatial distribution of the specific types of keypoints.

4.3. Applications of the proposed framework

In this section we will present a few possible applications of the proposed framework. The idea is to formulate a proof of concept, that the current framework can be used in object extraction and recognition tasks in computer vision. We will begin with the idea of extracting the shapes from an image using the topological notion of cover.

4.3.1. Persistence of Čech Shapes

One of the major themes in this article is to develop a topological framework for covers of an object in a digital image. The idea of using simple geometrical objects to cover a topological space, so as to extract topological and geometrical information about it dates back to Poincarě (Poincaré, 1895). The objects used here are disks (here called Čech balls), parameterized by the location of centers and radii. An important question that arises here is related to the choice of these parameters.

We choose the centroids to be the keypoints contributed by either SIFT or by hole based keypoints of Alg. 2. As to the choice of radii goes, we will use a recently developed technique, called persistent topology (Edelsbrunner & Harer, 2010), which is aimed at filtering out noise. The idea is that as we increase the radius of the Čech balls we get a new Čech complex which is a superset of the previous one. This can be written as: $for\,all\, r, s \in \mathbb{R}, r < s \Rightarrow cx_r \subseteq cx_s$. Here cx_r is a Čech complex yielded by Čech balls of radius r. This means that we get a filtration of Čech complexes indexed by the radius. Since, the question under investigation is the quality of a cover of the objects in digital images, we will employ appropriate measures in this regard.

The two measures that we use are the fraction of the area of the object covered by the Čech complex and the fraction of the area of Čech complex that lies on the object in the image. We want to cover the maximum area of the object while reducing the area of the background(parts of an image that are not the object), in the resulting cover. This is a trade off, which can be seen from Figs. 13.1 and 13.2. In Fig. 13.1 all of the Čech complex lies on the object, but it only covers a small area of the object. In Fig. 13.2, we are covering a significant portion of the object area, but the spillage into the background is also present. We need to strike a balance between the two parameters to attain a cover of the object that is well suited to approximating its geometrical and topological features. Hence, we plot the normalized values(on the range $[0, 1]$) of the measures for the whole filtration in the plot shown in Fig. 13.3.

From this plot we can decide upon the appropriate value of the radii for the Čech balls, which will suite our application. If the objective is to maximize the area of the object covered we would like the radius to be in the range of $170 - 220$, but the spillage of the complex would be significant. Another possible choice could be the intersection point of the two curves, which would yield a value of 120 for the radius. This perspective gives us a view of the topological and geometrical properties of the object, indexed by scale. Other possible extensions of this method could be, to consider indexing by the number of keypoints or to index by both the number of keypoints and the radius.

4.3.2. Shapes of Bird Species

Let us consider another application of the concepts developed in this article. We will consider the identification of different species of birds, based on their shape. The aim like the previous

13.1: Čech Complex with $\epsilon = 50$

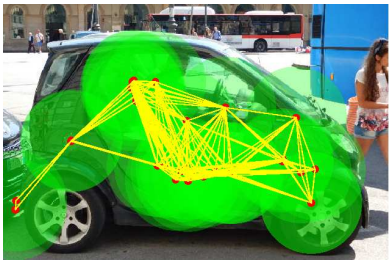

13.2: Čech Complex with $\epsilon = 150$

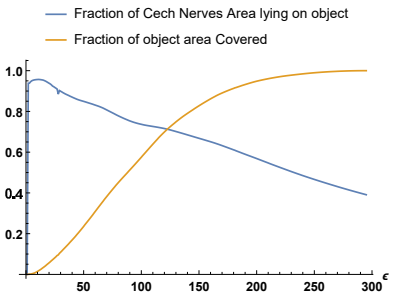

13.3: Persistence of Čech shapes

Figure 13. This figure illustrates the change in the area of the object covered by the Čech complexes of varying diameters,ϵ. The plots illustrate the fraction of the object area covered by the Čech complexes and the fraction of the complex area that lies on the object of interest.

application is to demonstrate the viability of the theoretical framework. For this purpose we select the database used in (Lazebnik *et al.*, 2005). We select three images of birds belonging to three different species. On the images we perform an analysis similar to the one detailed in Sec. 4.2.

We use the holebased keypoints as they take into account the description of the image(in terms of the locations of constant pixel intensity regions). This will be a crucial feature in the classification of different patterns. The patterns inside an object and the shape of its contour are some of the most important features when it comes to classification in computer vision. This can be understood by looking at the pictures of the three birds we aim to classify, shown in Figs. 14.1,14.4 and 14.7. These differ not only in terms of the shapes of their boundary contours but the patterns on them. For each of the birds, the Čech complexes formed by considering the holebased keypoints determined using Alg. 2, are shown in Figs.14.2,14.5 and 14.8. We can see that the 1-skeleton of the Čech complex (i.e. all the 1-simplices in it) conforms to the shape of the bird. An additional point to note here is that, it represents the proximity of the centroids of the regions with different descriptions. Hence, it is a more structural representation of the bird in terms of the regions of matching description in it.

For this example we resort to looking at the Čech spectra(Def. 20) of each of the images. This is the number of Čech nerves of different order in the image. Each of the Čech Nerves is itself a hyper-connected space, as it is a intersection of varying number of Cech balls. The order of the hyper-proximity is the same as the cardinality of the nerve. Hence, the Čech spectra can be equivalently thought of as the number of hyper-connected subspaces of different order in the image. The Čech spectra for the images of the three birds are show in Figs.14.3,14.6 and 14.9. It can be seen that the Čech spectra for the three birds are significantly different, hence providing a possible feature for classification.

4.3.3. Shapes of Butterfly Species

We present another application of the proposed framework to object detection for classification in computer vision. The aim is to provide a proof of concept, that the theoretical framework developed in this article can be used in practical applications. For this purpose, we aim to classify

14.1: Egret

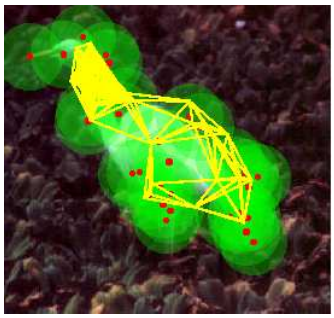

14.2: Čech Complex covering of Egret

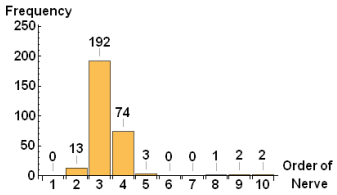

14.3: Čech Spectrum of Egret

14.4: Owl

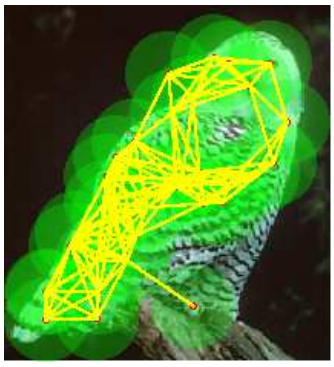

14.5: Čech Complex covering of Owl

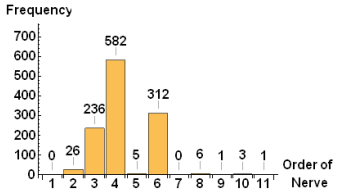

14.6: Čech Spectrum of Owl

14.7: Wood Duck

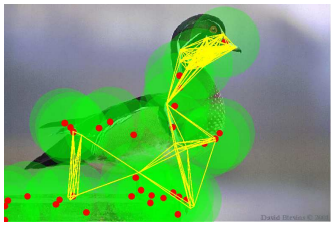

14.8: Čech Complex of Wood Duck

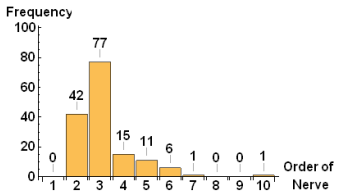

14.9: Čech Spectrum of Wood Duck

Figure 14. This figure illustrates the Čech complex coverings and the associated Cech spectra for images of three different birds taken from the database developed in (Lazebnik *et al.*, 2005).

butterflies based on their shapes. The dataset used in this task is taken from Lazebnik *et al.* (2004). We take three different images of butterflies belonging to different species. These images are shown in Figs. 15.1,15.4 and 15.7. All these butterflies are different from one another based on their shape and patterns.

As we discussed in the case of classifying bird species, a classifier that incorporates the pixel intensity description would perform better than the one that considers boundary contours alone. This fact becomes even more evident when we compare Figs.15.1 and 15.4, showing Black Snowtail and Machaon butterflies respectively. Both the butterflies have almost identical boundary

15.1: Black Snowtail

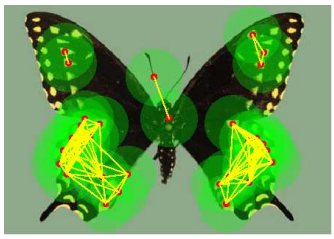

15.2: Čech Complex covering of Black Snowtail

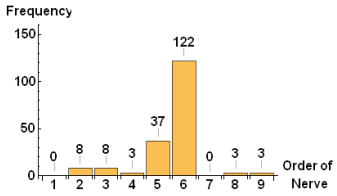

15.3: Čech Spectrum of Black Snowtail

15.4: Machaon

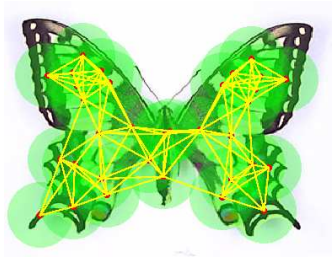

15.5: Čech Complex covering of Machaon

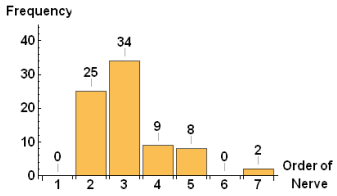

15.6: Čech Spectrum of Machaon

15.7: Zebra Butterfly

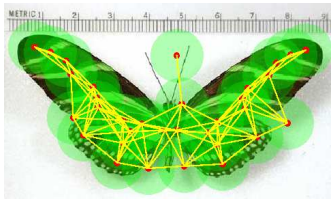

15.8: Čech Complex of Zebra Butterfly

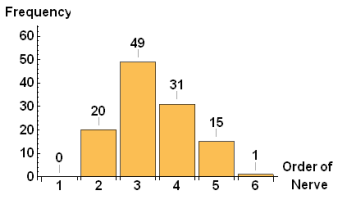

15.9: Čech Spectrum of Zebra Butterfly

Figure 15. This figure illustrates the Čech complex coverings and the associated Cech spectra for images of three different butterflies taken from the database developed in (Lazebnik *et al.*, 2004).

contours but differ drastically in terms of patterns. Thus, we must use the holebased keypoints calculated using Alg. 2, which are centroids of regions with matching description(in this case [pixel intensities). The methodology used here is similar to the Secs. 4.2 and 4.3.2. The Čech covers of the different butterflies are shown in Figs. 15.2,15.5 and 15.8. It can be seen that the difference of patterns dictates the locations of the holebased keypoints. It leads to different Čech complexes for both the Black Snowtail(Fig. 15.1) and the Machaon(Fig. 15.4). Moreover, the 1-skeletons(all the 1-simplices) of the Čech complexes conform to the structure of the shape.

Now to exploit this difference in the Čech complexes we use Čech spectrum(Def. 20) as a measure. The relationship between the Čech spectrum and hyper-connected subspaces of the image has been detailed in Sec. 4.3.2. We can see that Čech spectra for the different butterflies as shown in Figs.15.3,15.6 and 15.9 are substantially different. This difference elucidates the possibility of classification.

5. Conclusion

This paper uses proximal Čech complexes to approximates the shape of objects in digital images. Several topological structures with closed geometric balls as the primitive are formulated to study the geometrical and topological properties of objects. Moreover, instead of considering only the boundary contours of the object we also include the interior of the shape using descriptive proximity relations. The classical notion of proximity as a relation on two subsets has been extended to functions over arbitrary number of subsets. Moreover, the usual binary proximity is also extended to a continuous valued function also yielding the extent of nearness between objects. We define the concept of a descriptive hole in an image as a finite bounded region with a matching description. These are then used to formulate an algorithm to extract keypoints from an image. The distribution of the orders f the different Čech nerves in the image is used to define a signature for the shape of an object in digital images. The results for the computational experiments along with the algorithms used have also been presented.

References

A-iyeh, E and James Peters (2016). Rényi entropy in measuring information levels in voronoï tessellation cells with application in digital image analysis. *Theory and Applications of Mathematics & Computer Science* **6**(1), 77–95.

Ahmad, M.Z. and J.F. Peters (2017*a*). Delta complexes in digital images. Approximating image object shapes. *arXiv* **1706**(04549v1), 1–18.

Ahmad, M.Z. and J.F. Peters (2017*b*). Geodesics of triangulated image object shapes. approximating image shapes via rectilinear and curvilinear triangulations. *arXiv preprint arXiv:1708.07413*.

Alahi, Alexandre, Raphael Ortiz and Pierre Vandergheynst (2012). Freak: Fast retina keypoint. In: *Computer vision and pattern recognition (CVPR), 2012 IEEE conference on*. Ieee. pp. 510–517.

Alexandroff, P. (1965). *Elementary concepts of topology*. Dover Publications, Inc.. New York. 63 pp., translation of Einfachste Grundbegriffe der Topologie [Springer, Berlin, 1932], translated by Alan E. Farley , Preface by D. Hilbert, MR0149463.

Aubry, Mathieu, Ulrich Schlickewei and Daniel Cremers (2011). The wave kernel signature: A quantum mechanical approach to shape analysis. In: *Computer Vision Workshops (ICCV Workshops), 2011 IEEE International Conference on*. IEEE. pp. 1626–1633.

Borsuk, K. (1948). On the imbedding of systems of compacta in simplicial complexes. *Fund. Math.* **35**, 217?234.

Bronstein, Michael M and Iasonas Kokkinos (2010). Scale-invariant heat kernel signatures for non-rigid shape recognition. In: *Computer Vision and Pattern Recognition (CVPR), 2010 IEEE Conference on*. IEEE. pp. 1704–1711.

Bruna, Joan and Stéphane Mallat (2013). Invariant scattering convolution networks. *IEEE transactions on pattern analysis and machine intelligence* **35**(8), 1872–1886.

Carlsson, Gunnar, Afra Zomorodian, Anne Collins and Leonidas J Guibas (2005). Persistence barcodes for shapes. *International Journal of Shape Modeling* **11**(02), 149–187.

Čech, E. (1966). *Topological Spaces*. John Wiley & Sons Ltd.. London. fr seminar, Brno, 1936-1939; rev. ed. Z. Frolik, M. Katětov.

Chazal, Frédéric, David Cohen-Steiner, Leonidas J Guibas, Facundo Mémoli and Steve Y Oudot (2009). Gromov-hausdorff stable signatures for shapes using persistence. In: *Computer Graphics Forum*. Vol. 28. Wiley Online Library. pp. 1393–1403.

Edelsbrunner, H. and J.L. Harer (2010). *Computational Topology. An Introduction*. American Mathematical Society. Providence, R.I. xii+110 pp., MR2572029.

Ghrist, Robert (2008). Barcodes: the persistent topology of data. *Bulletin of the American Mathematical Society* **45**(1), 61–75.

Ghrist, Robert W (2014). *Elementary applied topology*. Createspace.

Hettiarachchi, Randima, James Peters and Neil Bruce (2014). Fence-like quasi-periodic texture detection in images. *Theory and Applications of Mathematics & Computer Science* **4**(2), 123–139.

Lazebnik, Svetlana, Cordelia Schmid and Jean Ponce (2004). Semi-local affine parts for object recognition. In: *British Machine Vision Conference (BMVC'04)*. The British Machine Vision Association (BMVA). pp. 779–788.

Lazebnik, Svetlana, Cordelia Schmid and Jean Ponce (2005). A maximum entropy framework for part-based texture and object recognition. In: *Computer Vision, 2005. ICCV 2005. Tenth IEEE International Conference on*. Vol. 1. IEEE. pp. 832–838.

Lowe, D.G. (1999). Object recognition from local scale-invariant features. In: *Proc. 7th IEEE Int. Conf. on Computer Vision*. Vol. 2. pp. 1150–1157. DOI: 10.1109/ICCV.1999.790410.

Peters, J.F. (2007*a*). Near sets. General theory about nearness of sets. *Applied Math. Sci.* **1**(53), 2609–2629.

Peters, J.F. (2007*b*). Near sets. Special theory about nearness of objects. *Fundamenta Informaticae* **75**, 407–433. MR2293708.

Peters, J.F. (2014). *Topology of Digital Images - Visual Pattern Discovery in Proximity Spaces*. Vol. 63 of *Intelligent Systems Reference Library*. Springer. xv + 411pp, Zentralblatt MATH Zbl 1295 68010.

Peters, J.F. (2017*a*). Proximal planar shapes. correspondence between shape and nerve complexes. *arXiv preprint arXiv:1708.04147*.

Peters, J.F. (2017*b*). Proximal planar Čech nerves. an approach to approximating the shapes of irregular, finite, bounded planar region. *arXiv preprint arXiv:1704.05727v4*.

Peters, J.F. and E. İnan (2016). Strongly proximal edelsbrunner-harer nerves. *Proceedings of the Jangjeon Mathematical Society* **19**(3), 563–582.

Poincaré, Henri (1895). Analysis situs. *J. de l'Ecole Poly.*

Segal, Jack and Jerzy Dydak (1978). *Shape theory*. Springer Verlag.

Shamir, Lior (2013). Unsupervised detection of outlier images using multi-order image transforms. *Theory and Applications of Mathematics & Computer Science* **3**(1), 13.

Smirnov, Yu. M. (1952). On proximity spaces (russian). *Mat. Sbornik N.S.* **31**(73), 543574. MR0055661; appears in AMS Translations, Series 2, volume 38, 1964, pp. 5-36.